FABRICATION AND CHARACTERIZATION OF ALUMINUM METAL MATRIX COMPOSITES USING RARE EARTH METAL AS AN ADDITIVE

A Thesis submitted in Fulfillment of the Requirement for the Award of the Degree of

MASTER OF ENGINEERING

in Production Engineering

Submitted By

DIVYANSHU AGGARWAL

801685006

Under Supervision of

Dr. Vinod Kumar
Associate Professor
&
Dr. R.S. Joshi
Assistant Professor

MECHANICAL ENGINEERING DEPARTMENT

THAPAR INSTITUTE OF ENGINEERING AND TECHNOLOGY

(A DEEMED TO BE UNIVERSITY), PATIALA, PUNJAB

JUNE, 2018

DECLARATION

I, Divyanshu Aggarwal hereby declare that the work presented in this thesis entitled "Fabrication and characterization of aluminum metal matrix composites using rare earth metals as an additive" in fulfillment of the requirement for the award of degree of Master of engineering (PE) submitted at Department of Mechanical engineering, Thapar institute of engineering and technology (Deemed to be University), Patiala is an authentic record of work carried out under supervision of Dr. Vinod Kumar (Associate Professor, TIET, Patiala) and Dr. R.S. Joshi (Assistant Professor, TIET, Patiala) from 2016 to 2018. The matter presented in this has not been submitted either in part or full to any other university or institute for the award of any degree.

Signature

Date: 14/07/2018

(DIVYANSHU AGGARWAL)

(801685006)

(Dr. Vinod Kumar)

(Associate Professor)

Dr. R.S. Joshi

(Assistant Professor)

Department of Mechanical engineering

Thapar institute of engineering and technology

(A Deemed to be University), Patiala, Punjab

ACKNOWLEDGEMENT

I would like to express my deepest sense of gratitude and a very sincere thanks to my guide **Dr. Vinod Kumar**, Associate Professor & **Dr. R.S. Joshi**, Assistant Professor Mechanical Engineering Department, Thapar institute of engineering and technology, Patiala for his sincere and invaluable guidance and full support which helped me in the accomplishment of this thesis report in present form. His dynamic and diligent enthusiasm has been highly instrumental in keeping my spirits high. His flawless and forthright suggestions blended with an innate intelligent application have crowned my task with success.

I am also thankful to **Dr. T.P. Singh**, Head of Department, Mechanical Engineering, for providing us with the adequate infrastructure in carrying out the work. I would like to thank the entire faculty and staff of Mechanical Engineering Department and my friends who devoted their valuable time and help me in all possible ways towards successful completion of this work. I thanks all those who have contributed directly or indirectly to this work.

Lastly, I would like to thank my family for their years of guidance, support, and encouragement. It would not have been possible without them to reach up to this point. They have always wanted the best for me and I admire their determination and sacrifices.

DIVYANSHU AGGARWAL

801685006

ABSTRACT

In this technological era, the demand of advanced engineering applications has been increased on a rapid rate. Need of the advance materials that can provide better mechanical properties, amenability to conventional processing technique and possibility in reducing production cost are the major demands of today's industrial world. Aluminum hybrid composites are the new generation metal matrix composites that have the potential to satisfy these demands.

The present study deals with the fabrication of aluminum metal matrix composites reinforced with Al_2O_3 + SiC and rare earth metal (CeO_2) as an additive. Improvement in the mechanical as well as tribological properties was examined. The mechanical properties such as hardness, tensile strength, percentage elongation along with tribological properties such as wear rate were examined. The microstructure analysis was done with the help of SEM, XRD and EDS techniques. The weight percentage of reinforcements used was a mixture of 5%, 10%, 15% (Al_2O_3 + SiC) and the rare earth metal used was 0.5, 1.5 and 2.5 weight %. The specimens selected for wear test were those having highest hardness values in both the cases i.e. non-rare as well as rare earth composites against base matrix alloy. The wear testing was done on a pin-on-disc tribometer using 10×12 mm composite pins against EN31 steel disc. Wear rate was examined against different sliding velocities i.e. 0.5, 1, 2 m/sec at different normal loads i.e. 10, 20, 30N. Progressive wear rate was also calculated at different sliding distances i.e. 500, 1000, 1500 and 2000 m. Microstructure of the wear specimens after the test was done with the help of SEM technique. It was observed that as the wear rate decreased with increase in value of sliding velocity and decrease in value of loads. The progressive wear shows a steady wear rate as the value of sliding distance increased. SEM images of the wear specimens shows the improvement in the surface texture by reduction in size of cracks and various other defects by addition of rare earth metal. The hardness, tensile strength and percentage elongation of the composites also increased with the increase in % reinforcements but as compared to non-rare earth composites, the composites having rare earth metal as an additive shows better enhancement in properties as compared to non-rare earth composites whether mechanical or tribological. The microstructure analysis shows better refinement of the composite after addition of rare earth. XRD and EDS analysis shows successful incorporation of hybrid composite particles.

TABLE OF CONTENTS

LIST OF TABLES

LIST OF FIGURES

NOMENCLATURE

MMC	Metal matrix composites
UTS	Ultimate tensile strength
AMMC	Aluminum metal matrix composites
YS	Yield Strength
BHN	Brinell hardness number
SiC	Silicon Carbide
B_4C	Boron Carbide
MoS_2	Molybdenum disulphide
rGO	reduced Graphene Oxide
GNSs	Graphene Nanosheets
TiB_2	Titanium di boride
ZrO_2	Zirconium oxide
ZnO	Zinc oxide
TiO_2	Titanium dioxide
GO	Graphene oxide
MWCNT	Multiwall carbon nanotube
CTE	Coefficient of thermal expansion
Er	Erbium
Zr	Zirconium
Eu	Europium
WC	Tungsten carbide
Gr	Graphite
CeO_2	Cerium oxide
DRA	Discontinuously reinforced Aluminum
Sb_2S_3	Stibnite
FA	Fly ash
SiC	Silicon carbide
BLA	Bamboo leaf ash
B_4C	Boron carbide

Chapter 1

Introduction

1.1 General Introduction

In the era of globalization, the demand of new products with advanced materials and process technologies is increasing. Stronger, lighter, and less expensive materials are current requirement of engineering applications. Metal matrix composites (MMCs) offer such properties required in a wide range of engineering applications. MMCs are metallic alloys that are reinforced with various types of reinforcement materials and especially ceramic materials [1]. Most of these properties include: high specific strength, lower coefficient of thermal expansion and high thermal resistance, excellent wear resistance, high specific stiffness and superior level of corrosion resistance [2-4]. Light metals alloys such as Al, Mg and Ti are the common metallic alloys utilized today. Metal matrix composites are the composites with at minimum of two constituent parts, one of which is a metal which is necessary; another material can be a different metal or a material such as organic compound or ceramic.

1.2 Manufacturing and forming methods

Metal matrix composites can be manufactured by various techniques which are divided into three classes i.e. solid, liquid and vapor.

1. Solid state methods
2. Liquid state method
3. Semi-solid state method
4. Vapor deposition
5. In-situ fabrication technique

1.2.1 Solid State methods

Solid state methods consists of methods such as

- Powder blending is a method which consists of mixture of powdered metal and discontinuous reinforcements and then they are bonded by a process of compaction.
- Foil diffusion bonding method consists of metal foil layers that are sandwiched along with long fibers, and then forms a matrix by through pressing.

1.2.2 Liquid state methods

It consists of

- Electroplating and electroforming
- Stir casting
- Pressure infiltration
- Squeeze casting
- Spray deposition

1.2.3 Solid state methods (semi)

It consists solid powder processing in which heating of powder mixture is done upto semi-solid state and further composites are formed by applying pressure.

1.2.4 Vapor Deposition

It consists of vapor deposition in which a coated fiber is passed through a thick cloud of vaporized metal.

1.2.5 In-situ fabrication method

It consists of a unidirectional solidification of a eutectic alloy in a controlled form, which results in a two-phase microstructure i.e., present in fiber form and distributed in the matrix.

The alloys are coded and various series of codes are available according to which the selection of alloys are done. A four digit number is given to each alloy, where the first digit represents the major alloying elements; the second digit indicates (if different from 0) represents variation of the alloy and the third and fourth digit identifies the series of specific alloy. The various types of aluminum alloy series are shown below.

Table 1.1 Aluminum alloy series

SERIES	COMPOSITION
1000	99% pure aluminium
2000	Al + Cu
3000	Al + Mn
4000	Al + Si
5000	Al + Mg
6000	Al + Mg + Si
7000	Al + Zn
8000	Other elements along with Al

Aluminum metal matrix composites (AMCs) are one of the most common and widely used materials in the industrial world today. AMCs are widely used in aerospace, automobiles, defense etc. [5]. AMCs show excellent mechanical properties, low distortion and excellent weldability [6]. Most of the reinforcements used in the aluminum matrix are SiC, $Al_2 O_3$, B_4C, TiC, TiB_2, MgO, TiO_2.

The reinforcements in the AMCs are in the form of continuous or discontinuous fibres, whiskers or particulates in volume which has a range from few percentages to 70% (3). The different reinforcements used in the formation of AMCs can be classified as ceramic particulates, industrial wastes, agro wastes and reinforcements with traces of rare earth elements [1, 7, and 8]. Reinforcements are mainly added to enhance the properties of base metal like strength, stiffness, conductivity etc. Stability of reinforcement is necessary in the given temperature and non-reactive too. Silicon carbide (SiC) and aluminum oxide (Al_2O_3) are the most commonly used reinforcements. SiC reinforcement improves the properties like tensile strength, hardness, density, and wear resistance of Al and its alloy. The distribution of particles plays a very important role in the properties of Aluminum MMCs. Al_2O_3 reinforcements have good compressive strength and wear resistance. Boron carbide is one of the hardest elements known. It has high value of elastic modulus and fracture toughness. The addition of boron carbide (B_4C) in aluminum matrix increases the hardness but does not improve the wear resistance much [15].

AMC materials provide a better combination of properties in such a way that today none of the existing monolithic material could offer. From many years AMCs are used in numerous structural, non-structural and functional applications in different engineering sectors. The driving force needed for the utilization of AMCs in these sectors include performance, economic as well as environment benefits. (3)

1.3 Types of AMCs (3)

AMCs can be classified in four different categories depending on the type of reinforcements

1. Particle reinforced aluminum metal matrix composites (PAMCs)
2. Whisker and short fiber reinforced AMCs (SFAMCs)
3. Continuous fiber reinforced AMCs (CFAMCs)
4. Mono filament reinforced AMCs (MFAMCs)

These are explained as below

1.3.1 Particle reinforced aluminum metal matrix composites (PAMCs)

PAMCs consist of equally distributed ceramic reinforcements with an aspect ratio of < 5. Ceramic reinforcement are either oxides, carbides or borides (i.e. Al_2O_3 , SiC, TiB_2) and available in volume fraction of < 30% when used for applications of wear resistance and structural. PMACs are manufactured in two ways, either by using solid state (Powder metallurgy) or liquid state (Stir casting, infiltration) processes. Mechanical properties of PMACs are better compared to SFAMCs.

1.3.2 Whisker and short fiber reinforced AMCs (SFAMCs)

SFAMCs contain reinforcement with an aspect ratio of > 5, but are continuous. Short alumina fiber reinforced aluminum matrix composites are the very popular AMCs to be developed and used in automobile parts such as pistons. Squeeze infiltration process is used for their production. Mechanical properties of whiskers reinforced composites are mush superior than particle or short fiber reinforced composites.

1.3.3 Continuous fiber reinforced AMCs (CFAMCs)

In these composites the reinforcements are in the form of continuous fibers of alumina, SiC. AMCs which have fiber volume fraction upto 40% are produced by squeeze infiltration method. Recently corporation named 3M^{TM} has developed an alumina fiber (continuous fiber) reinforced composite with 60% volume and have a tensile strength of 1500 Mpa and elastic stiffness 240 Gpa. These composites are produced by pressure infiltration route.

1.3.4 Mono filament reinforced AMCs (MFAMCs)

These are having fibers with diameter (100 to 150 μm), usually produced by chemical vapor deposition (CVD). Bending flexibility of monofilaments is very low when compared to multi filaments. In CFAMCs and MFAMCs, the constituent that bears the major load is the reinforcement and role played by the aluminum matrix is to bond the reinforcement and transfer as well as distribute the load, whereas in the particle and whiskers the matrix is the load bearing constituent and reinforcement helps to strengthen and stiffen the composite by preventing matrix deformation by mechanical restraint.

1.4 Application of Aluminum MMCs

MMCs are replacing conventional metallic alloys quickly into so many applications. Their applications have been extended from aerospace and automobile, defense, marine, sports and recreational industries. Some of the widely used aluminum MMCs are listed below:

- Al/SiC = Pistons, Brake rotors, propeller shafts, connecting rod, brake disc, multiple electric module, PCB heat sinks, engine cradle, bicycle fork brakes, disc brake rotors,
- Al/ $Al_2 O_3$ = Piston rings, engine blocks, sprockets
- Al/Cu/Gr = current collectors, cylinders, pistons,
  Etc (10)

Chapter 2

Literature review

Literature provides a strong impression in relation to the scope as well as interest in the field of Aluminum metal matrix composites. Various aspects regarding the fabrication and different reinforcements used in Aluminum MMCs were addressed by pioneer researchers throughout the world.

Sijo M T, K R Jayadevan (11) (2016) investigated stir cast Al/SiC MMCs. A small description of various fabrication techniques was available in this study and stir casting route was considered as the simple, less expensive and can be used for mass production.

Table 2.1 A comparative study of various processing methods [11]

Method	**Range of shape And Size**	**Metal Yield**	**Range of volume fraction**	**Damage to Reinforcement**	**Cost**
Powder Metallurgy	Wide range, Size restriction	High	-	fracture of reinforcement	Expensive
Squeeze Casting	Limited by perform shape up to 2cm Height	Low	Upto 0.45	Intense damage	Moderate
Spray Casting	Limited shape, Large size	Medium	0.3 to 0.7	-	Expensive
Mechanical Stirring	No size limitations	Medium	0.4 to 0.7	Little damage	Moderate
Electromagnetic Stirring	No size limitations	High	0.5 to 0.8	No damage	Moderate

The study clearly showed mechanical properties of stir cast composite depend upon factors such as fabrication techniques, reinforcement particles size and shape, volume fraction and the distribution and properties of constituents.

Ritesh Raj, Dineshsingh G. Thakur (12) (2016) presents a study of qualitative and quantitative assessment of microstructure in Al- B_4C MMC processed by modified stir casting technique. The author deals with processing of 6061Al-B_4C composites containing different weight percentages of B_4C and used modified stir casting method with bottom pouring arrangement. They used a two bladed stainless steel stirrer with

varying speed from 100-1500 rpm and a stainless steel crucible. The homogeneous and uniform distribution of particles in the matrix was observed.

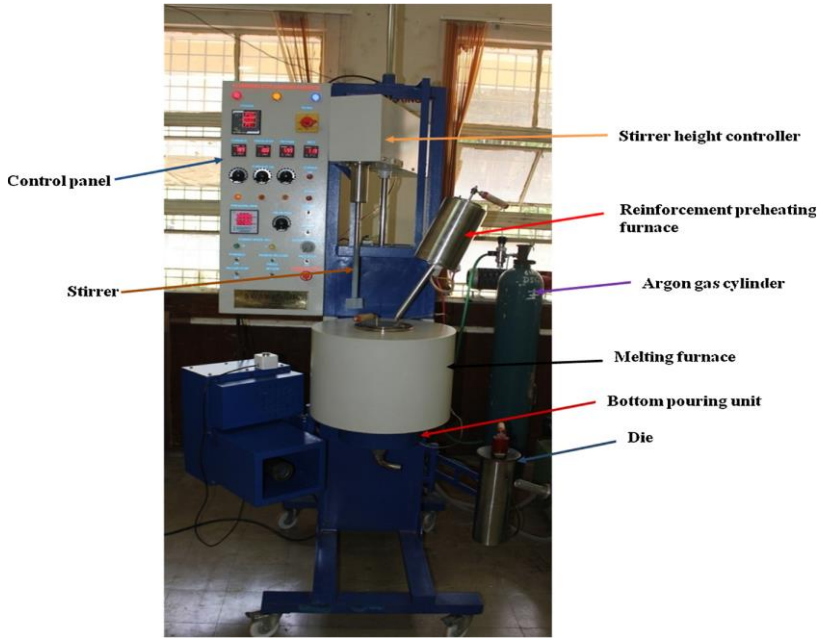

Figure 2.1: Modified stir casting machine setup [12]

Singh etal (13) (2017) presented as study on mechanical as well as microstructure behavior of Al6082-T6/SiC/B_4C based aluminum hybrid composites using conventional stir casting technique and different percentage of weight i.e. 5,10,15 and 20% of (SiC and B_4C mixture). It was concluded that the hardness value of reinforced alloy as compared to unreinforced alloy was increased by 10%, impact strength falls down gradually but the ultimate tensile strength was improved by 21% these all values increased till addition of 15 wt% of reinforcement but as the value reaches 20% sudden decrease in values take place.

H.S.Arora etal (14) (2013) investigated friction stir processed Mg alloy wear behavior. Pin-on-disc machine (using universal tribometer) was used for performing wear test. The wear rates were examined under various load conditions i.e. 5 to 20 N under different sliding velocities varying from 0.33 to 3 m/sec. SEM and XRD techniques were used for analyzing worn surface and wear debris. It was observed that the friction stir processed (FSPed) AE42 alloy showed noticeable decrease in the wear rate was observed, which was due to the microstructural refinement that results an increased hardness and ductility of the FSPed alloy. It was also observed by the author that maximum wear rate occurred at higher loads & lower velocities. The maximum wear mechanisms at higher velocities were found to be plastic deformation along with some part of delaminations.

Selvam etal (15) (2013) focuses on syntheses and characterization of Al6061/fly ash/SiC composites prepared by stir casting and compo-casting methods. The author used 7.5 to 10% of SiC along with constant amount of Fly ash i.e. 7.5% and concluded that there was an improvement in micro and macro hardness of the composite with the addition of fly ash from 69.53 HV to 78.8 HV and 49.4 BHN to 57.21 BHN and there was improvement in tensile strength of composite from 173 Mpa to 213 Mpa. The homogeneous dispersion of SiC and Fly ash was found in SEM micrographs.

Zhang etal (16) (2008) proposed a research on improvement of toughening mechanisms of alumina matrix ceramic composite material by adding mixed rare earth additive. Mixed rare earth used by the author were Nd, Ce, La and Pr. Different reinforcement percentage was used and it was concluded that Composites with 9.5 vol.% AlTiC, 0.5vol.% mixed RE and 90 vol.% alumina shows the bending strength, toughness and hardness were 617.6 MPa, 5.77MPa and 20.7 GPa. But when the percentage reaches above it i.e. 3% there was sudden decrease in properties of the composites.

P.S.Samuel Ratna Kumar etal (17) (2017) shows the corrosion behavior of aluminum metal matrix reinforced with multi wall carbon nanotube. Multi walled carbon nanotube having more than 98% purity, 5-20 nm diameter and 1-10µm average length was used with different compositions such as 1, 1.25, 1.5, 1.75 weight percentage to improve the corrosion behavior of aluminum nano metal matrix composites. The results shows that Hardness increased from 74 BHN for the alloy Al5083 to 84 BHN for 1.75 wt% of reinforced composite and corrosion resistance also increases at room temperature.

James etal (18) (2014) worked on the hybrid aluminum MMCs reinforced with SiC and TiB_2 with varying weight percentages of TiB_2 and constant value of SiC i.e.10%. The author concluded that with the addition of reinforcement the hardness value effected but with the addition of TiB_2 upto 5% leads to porosity which led to decrease in hardness value. Addition of SiC added 20% to the strength but addition of TiB_2 reduce strength to 50-60% also it increases the surface roughness.

Mohammad Hasan Shofaeefard etal (19) (2016) investigated the frictional stir casted Al356 matrix composite and the effect of reinforcement on its microstructure, mechanical properties and wear resistance. The reinforcements used were SiC, TiC, ZrO_2, B_4C with weight percentage of 12% each. The properties like hardness and wear test were measured and it was concluded that the composites reinforced with TiC particles exhibited higher hardness value as compared with other material. Wear resistance also

improved as compared to base material value. The plowing that occurred on the surface of Al-TiC and Al- B_4C composites caused due to wear shows that abrasive wearing takes place. However the composites reinforced with SiC and ZrO_2 have both abrasive and adhesive wear mechanism.

Bhargavi Rebba etal (20) (2014) evaluates the mechanical properties of aluminum alloy -2024 reinforced with molybdenum disulphide (MoS_2) metal matrix composites. The reinforcement used was in weight percentage of 1,2, 3, 4, 5 %. The author concluded that the values of hardness and tensile strength were increased upto the addition of 4% reinforcement but when the value reaches to 5% there was a sudden decrease in the values. SEM micrographs of the fractured tensile specimen revealed that the fracture was a ductile fracture.

Xu wang etal (21) (2011) presented the study on effect of Nd content on mechanical and microstructural properties of Gr/Al composites. M40 graphite fiber reinforced Al-17Mg matrix composite was used with different contents of Nd i.e. 0.2, 0.5, 2 weight percentage. Microstructure of the composite was observed by using various techniques like SEM, XRD, TEM, HRTEM. Various phases of $Al_{11}Nd_3$ and Al_3Mg_2 followed by segregation of Nd and Mg at carbon aluminum interface were also observed. It was concluded that with the increase in addition of Nd content in matrix there was sudden decrease in the bending strength of Gr/Al composites. There was decrease in pull-out of single fiber and bundles due to increase in Nd content.

K.R. Padmavathi etal (22) (2014) showed the tribological behavior aluminum hybrid metal matrix composites using SiC and multi walled carbon nanotube (MWCNT) as reinforcements. The base alloy used was Al-6061. SiC was used with fixed volume percentage of 15% and MWCNT with varying percentage of 0.5% and 1.0%. It was observed that specific wear rate decreases with the increase of the wt % of MWCNT. There was a sudden decrease in hardness value at 0.5% MWCNT but when the value reaches 2% the hardness value increases.

Sidesh Kumar etal (23) (2014) showed the mechanical and wear behavior of Aluminum MMCs using Al2219 as base alloy and B_4C and MoS_2 as reinforcements. The weight percentages taken were 3, 4, 5 % keeping B_4C at 3% constant. The author concluded that on increasing the %age of reinforcement density, hardness increases but tensile Strength and Yield Strength Decreases. The SEM images of Al2219 fractured surfaces shows

dimple patterns & the fractured surfaces of hybrid composites consists of both dimple patterns and tear ridges, this shows the ductility and brittle fracture of mixed mode.

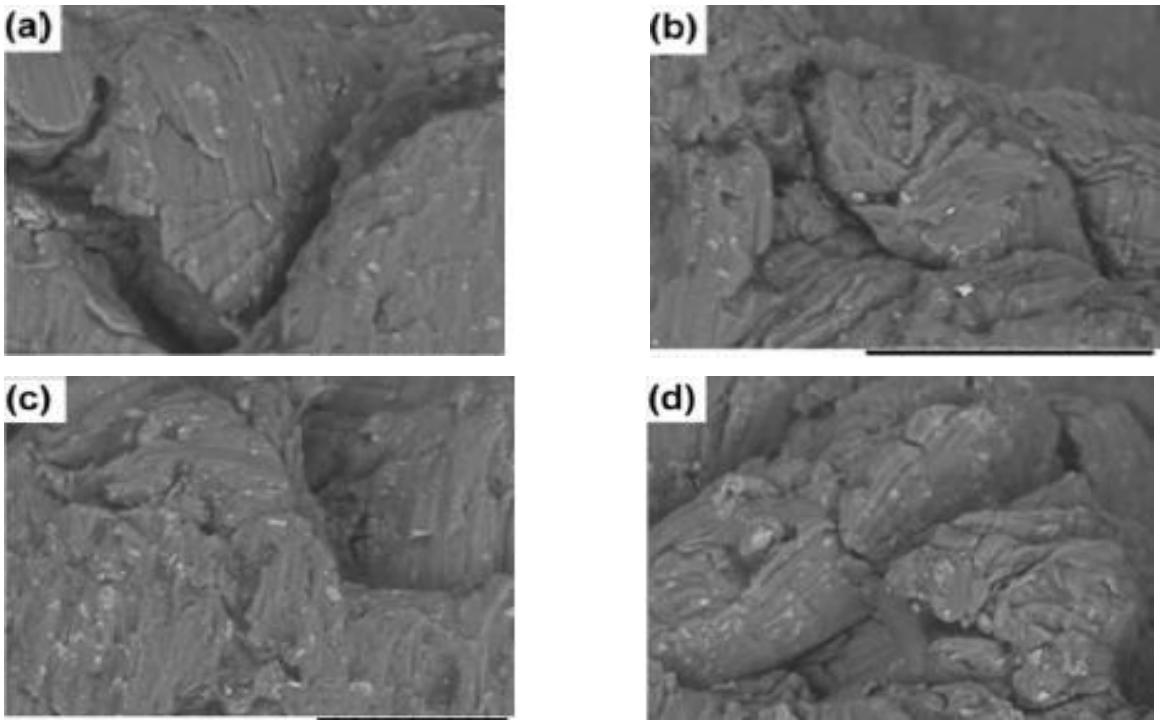

Figure 2.2 SEM Micrographs of fractured surface of (a) Al alloy (b) Al+3%B_4C+3% MoS_2 (c) Al+3%B_4C+4% MoS_2 (d) Al+3%B_4C+5% MoS_2 (23)

Manoj Kumar Pal etal (24) (2015) investigated the optimum composition and mechanical properties of Al/Ni MMCs. Specimens with 10, 20, 30 and 40% Ni were tested and 20% composition Ni specimen was considered as optimum. The BHN value of the specimen increased by 14.80%, Rockwell hardness increased by 2.43%, ultimate tensile strength increased by 1.003% and 24.98% decrease in thermal conductivity was observed as compared to aluminum.

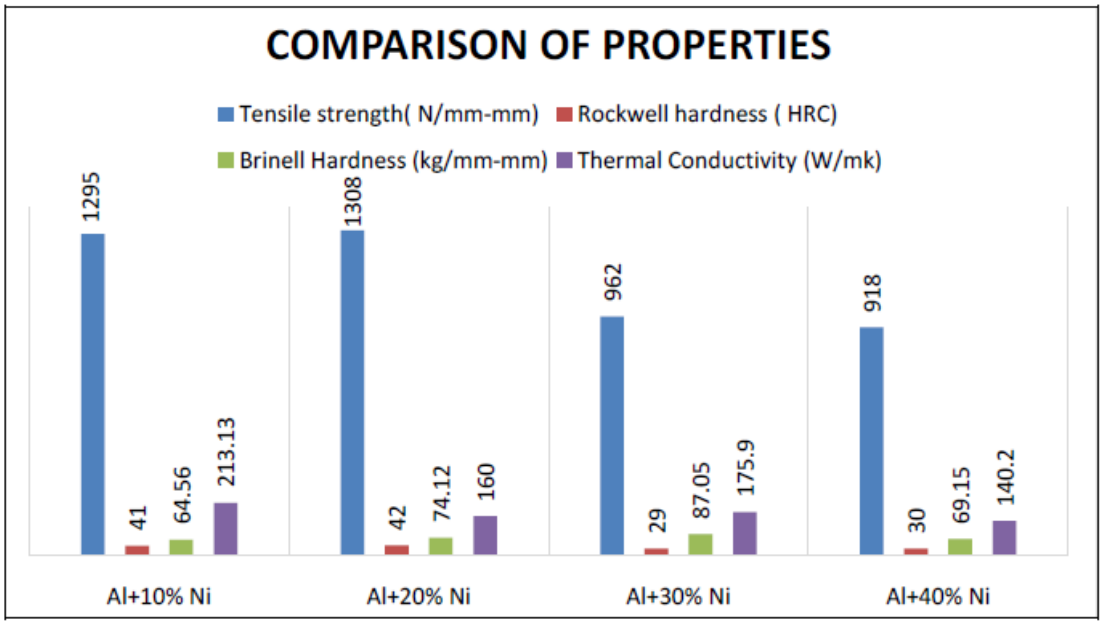

Figure 2.3: Graph showing the properties of composites in a nutshell (24)

Dora Siva Prasad etal (25) (2014) investigated the mechanical properties of Aluminum MMCs using rice husk ash (RHA) and SiC as reinforcement. Volume fraction of 2, 4, 6, 8 wt% in equal proportions was used. The author observed that there was an increase in the hardness and porosity of the composite with increase in reinforcement volume fraction and decrease in density with increase in content of particle. The UTS and yield strength also increased with increase in weight fraction whereas elongation decreases. The microstructure analysis was done with the help of SEM and XRD techniques.

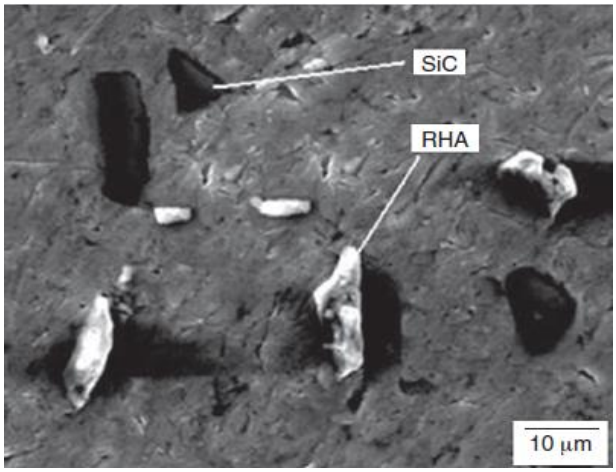

Figure 2.4 SEM of Al/RHA/SiC composite (25)

Prashantha Kumar H.G etal (26) (2017) investigated the mechanical and tribological properties of Al2024/SiC/Graphene hybrid composites. The author focuses on use of graphene to reduce the wear and frictional coefficient of Al2024/SiC/graphene reinforced composites. The weight percentage of graphene used was 0.5% and varying percentage of SiC was used as 4, 8, and 12%. The mixtures were then hot compacted and microwave sintered. Graphene and SiC content effects were evaluated in the composite under different conditions of normal load and disc speed using dry friction wear test on pin-on-disc tribometer. Surface roughness and microscopic studies were carried out on wear tracks. It was observed by the author that the wear loss, surface roughness, coefficient of friction values decreased due to presence of graphene and increased content of SiC. Improvement in tribological properties was also observed.

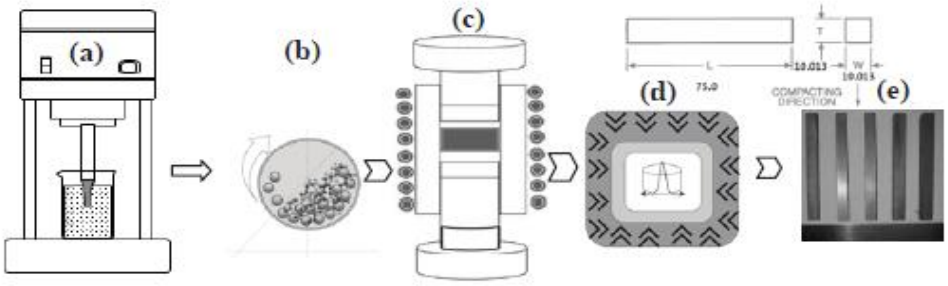

Figure 2.5: (a) Processing of powder by Ultrasonic liquid processor (b) Ball milling (c) Hydraulic press for uniaxial compaction of powder (d) Microwave sintering (e) Al2024-SiC-Graphene bar samples (26)

Hongying Li etal (27) (2013) investigated the effect on precipitation and recrystallization of pure aluminum by adding Er and Zr to it. The reinforced composites formed were Al-0.2Er-0.2-Zr and Al-0.2Er. The results showed that the recrystallization temperature of the Al-0.2Er-0.2-Zr (wt%) was about 450°C , which was significantly higher than Al-0.2Er (wt%) alloy (350°C).

F.S Rashed, T.S Mahmoud [28] presented artificial neural networks (ANN) approach to predict the wear behavior of A356/ SiC MMCs prepared using stir casting route. STATISTICA neural network software was used as optimization software. Multilayer perceptron (MLP) technique was used to develop ANN model. An MLP is a network of neurons called perceptrons. A single output is computed by perceptron from various multiple real valued inputs by forming a linear combination according to its input weights. Mathematically it was shown as

$$Y = \varphi \left(\sum_{i=1}^{n} \omega i x i + b\right)$$

Where,

ω denotes the weight vector, x is the input vector, b is the bias and φ is the activation function.

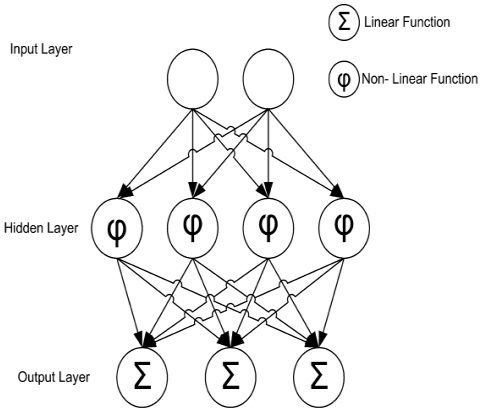

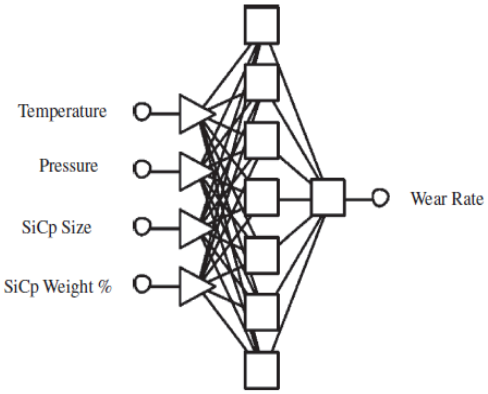

Figure 2.6: Signal flow model of an MLP network Figure 2.7: MLP ANN network

Cost and time could be easily saved by using ANN models. ANN approach is a successful method that can be used to predict the wear behavior of new materials and composites.

Jain R.K. etal (29) (2015) investigated the effect of input parameters on material removal rate (MRR), change in surface roughness (ΔRa), and surface topography by Taguchi method using L27 array which was designed for experimentation. Optimization of response surface parameters (MRR and ΔRa) was determined using the Taguchi method. Analysis of variance was done using MINITAB software. A proper taguchi combination was developed for both values of MRR & ΔRa.

Kiran kumar ekka etal (30) (2015) used both ANN and TAGUCHI methods were used as experimental techniques. The effects of percentage reinforcements, applied normal load, sliding speed and sliding distance on sliding wear behavior was investigated using Taguchi method. Both regression and ANN were used to predict the wear behavior and it was observed that prediction of ANN model was more efficient.

Fe Huang etal (31) (2017) numerically studied a 2D compaction of binary Al/SiC composite powder using a multi-particle finite element method (MPFEM). Different initial packing structures with various Al/SiC particle ratios and compositions were constructed and imported into FEM model for compaction. In the whole process, the macro and the micro properties of the compacts were monitored and characterized and the densification method was identified.

K. Soorya Prakash (32) (2016) investigated wear as well as mechanical behavior of Mg/SiC/Gr hybrid composites. The composites were prepared through powder metallurgy route. Following 8 composites were prepared

1. Mg
2. Mg-5SiC
3. Mg-10SiC
4. Mg-5Gr
5. Mg-10Gr
6. Mg-5SiC-5Gr
7. Mg-5SiC-10Gr
8. Mg-10SiC-5Gr
9. Mg-10SiC-10Gr

It was concluded by the author that an optimum increase in the density, wear resistance and micro-hardness of the magnesium was there with increase in SiC content. The addition of Gr improves the density and wear resistance but tends to reduce the micro-hardness. Mg-10Gr composite exhibits lower coefficient of friction whereas Mg-10SiC composite show higher coefficient of friction It was observed from SEM micrographs that the addition of Gr results in the brittle fracture of the surface and due to which composites reinforced with Mg-10SiC-5Gr shows better wear resistance as compared to Mg/10SiC/10Gr. Therefore author concludes that the optimum percentage of Gr solid lubricant should not be more than 5%.

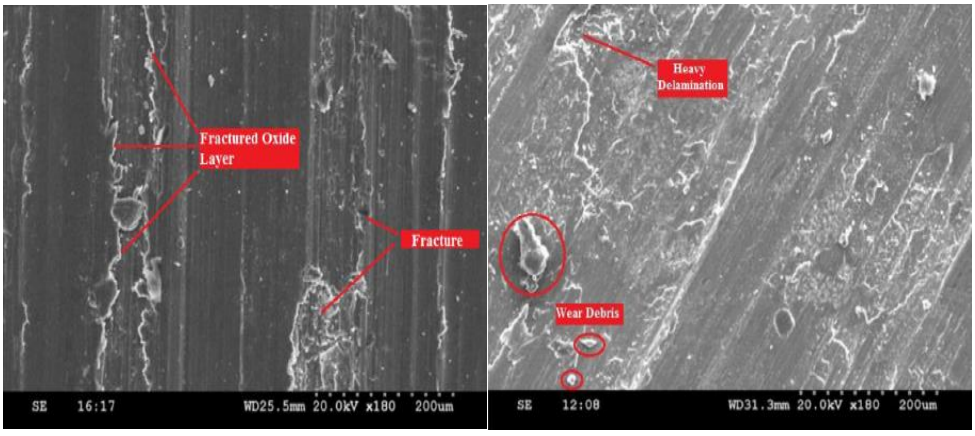

(a) (b)

Figure 2.8: SEM images of worn surfaces of (a) Mg/5SiC/5Gr, (b) Mg/10SiC/10Gr (32)

Vipin K. Sharma (33) (2017) investigated the effect of fly ash particles with aluminum melt on the wear of aluminum metal matrix composites. The weight percentage of fly ash used was 2-4-6% weight. It was concluded that the MMC with 6% weight of fly ash content results in less wear i.e. 0.32 gm and 4% weight of fly ash content gives the low coefficient of friction i.e. 0.12 between the tribo parts of cast iron surface and MMC surface. 6% weight of fly ash resulted in maximum average coefficient of friction i.e. 0.161. So the amount of fly ash content in the aluminum matrix was concluded to be kept upto 4%, more addition of fly ash increases the coefficient of friction between the triboparts.

Youming Liu etal (34) (2004) investigated effects and behavior of rare earth CeO_2 on in-situ TiC/Al composite. It was concluded by the author that an addition of 0.5 weight % addition of CeO_2 promotes the generation and refinement of TiC particles, prevents the formation of Al_3Ti, increase the wettability between the TiC particles and the Al matrix as well as improvement in the mechanical properties of the composites was observed.

Chapter 3

Research Gaps and Problem formulation

3.1 Introduction

This chapter covers the detailed objective of the proposed research work. It presents the overall objective of the proposed research, methodology, and experimental procedure to be adopted. The objectives of the research are set by keeping n mind the research gap in literature.

3.2 Research gaps

The study of hybrid composites has become very popular research nowadays. The researchers and academicians have worked and explored various types of hybrid composites with different type of compositions of reinforcements in them just to develop a low cost, high strength composite material for different purposes. Various tests have been conducted on them so as to achieve good mechanical as well as tribological properties.

The present literature survey reported gaps and limitations which are mentioned as below

1) Various researches showing improvement of Bending strength, hardness using Al alloy and SiC & Al_2O_3 as reinforcement are done but very few researches have been done to improve the ductility of the material. So in order to improve ductility of material rare earth can be bring into use as future material for research.
2) Various research have been carried out utilizing SiC, TiC, Al_2O_3, Gr, B_4C, CaC_2 alone or combining with various Al alloys to investigate the mechanical properties and observing the composite structure, but till date a very few researches have been carried out on Al 6061 reinforced with mixture of ($Al_2O_3 + SiC$) and rare earth element CeO_2 (Cerium oxide) as an additive.
3) Very limited amount of work has been carried out on enhancement of tribological properties of Al MMCs with rare earth additive.

3.3 Formulation of the objectives

The main objective of the proposed research work is to develop an aluminum metal matrix composite which can show better mechanical and tribological properties with the addition of rare earth elements. As it can be observed from the literature review that there is limited use of rare earth as an additive in alumina MMCs fabrication and also it was observed that there was no such fixed composition of adding rare earth in the matrix mentioned because of which it was not possible to examine the correct value of weight percentage of rare earth addition. The main focus of the present research work was to analyze the maximum value of rare earth addition upto which the hardness of the material can be increased as well as comparing the mechanical and tribological properties of the rare earth composites with non-rare earth composites and the base alloy. Also to fabricate a composite of Al MMC along with rare earth addition on which very little research have been done.

Chapter 4

Methodology

4.1 Introduction

This chapter provides the step wise procedure which is used to accomplish the research objectives, the plan of work was started with the selection of materials through literature review and then fabrication of composites. The detailed methodology for the proposed work comprises of two main phases.

Phase 1

In the first phase is the selection of matrix material and the reinforcement which was carried out such that their compatibility has no issue and satisfies the proposed objectives. Materials selected were such that the desired properties would be achieved.

Phase 2

In the second phase of work, fabrication of composites was been carried out and afterwards characterization in terms of microstructural analysis, mechanical testing, tribological behavior of the composites was studied. The fabrication of the composites was done with the help of stir casting technique. Techniques such as Scanning electron microscopy (SEM), X-ray diffraction, and energy dispersive spectroscopy were utilized for studying the microstructure and properties of composites. Micro and macro hardness were carried out in order to study the effects of reinforcements on the composites. Dry sliding wear test was conducted at varying speeds and sliding distances. Further, normal load was varied to study the effects of load on wear phenomenon.

4.2 Material Selection

In the literature a complete overview is reported for different matrix alloys and reinforcements combinations. Selection of the material is done on the basis of objectives decided to be achieved. It is basically based in the desirable properties of any component under its functional environment. The material used for the study should be stable in the given working temperature and non-reactive too. On the basis of objectives Aluminum 6061 alloy was considered as base matrix alloy and the chemical composition and mechanical properties of the matrix alloy are shown in table 4.1 and 4.2.

Table 4.1 Chemical composition of Al6061 alloy (wt%)

ELEMENT	Mg	Si	Cu	Zn	Ti	Mn	Cr	Al
AMOUNT (Weight %)	0.84	0.69	0.22	0.07	0.05	0.30	0.08	Balance

Table 4.2 Mechanical properties of Al6061 alloy

UTS (Mpa)	Proof Stress (0.2% Mpa)	Density (g/cm^3)	Vicker Hardness (HV)	Brinell Hardness (HB)	% Elongation
105-152	65-110	2.7	64.9	30-33	9

4.2.1 Selection of reinforcement

The selection of reinforcement is done considering the objectives to be fulfilled. The reinforcement should be non-reactive and stable in the given working temperature. The most commonly used reinforcements are SiC and Al_2O_3. According to literature survey SiC tends to increase tensile strength, density, hardness and wear resistance of the Al alloy, whereas Al_2O_3 provide good compressive strength and wear resistance. So these reinforcements were selected for the present research work along with a rare earth metal i.e Cerium oxide (CeO_2) as an additive. Magnesium (1%) was used as the wetting agent so as to increases the wettability of the reinforcement with the matrix alloy. The details of the reinforcements used for the work are shown in table 4.3

Table 4.3 Properties of SiC, Al_2O_3 and CeO_2 particles

Reinforcement	Average particle size (µm)	Density (g/cm^3)	Melting point (°C)
Al_2O_3	40	3.95	2,072
Sic	220	3.20	2,700
CeO_2	5	7.22	2,400

SEM images of the reinforcement powders are shown in figure. The images shows that the particles of Al_2O_3 and SiC are very hard in nature and can provide good corrosion resistance to the base alloy. Also with the addition of Al_2O_3 and Sic powders the hardness and wear resistance of the composite can also be enhanced. CeO_2 particles image shows some branched chain non-uniform structures.

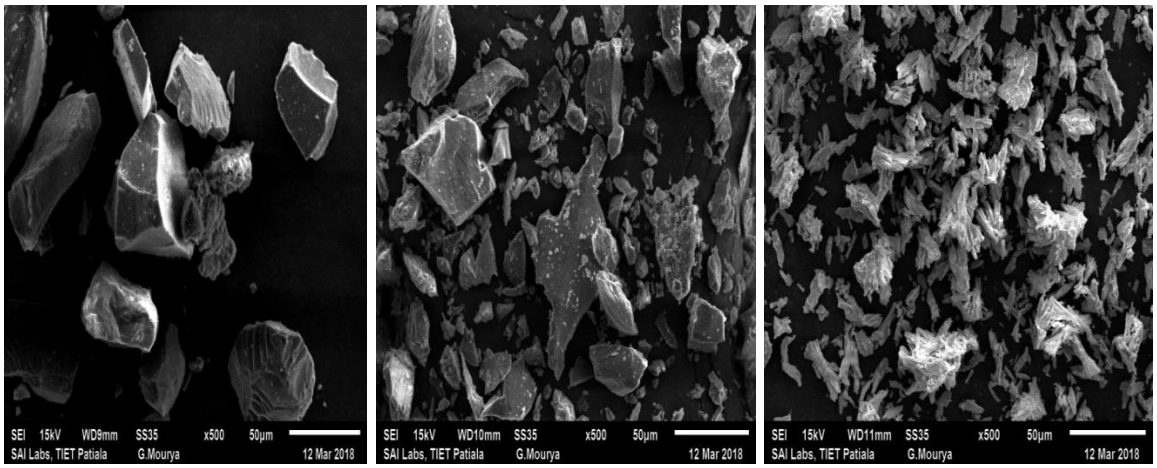

(a) (b) (c)

Figure 4.1: SEM images of (a) Al_2O_3 powder (b) SiC powder (c) CeO_2 powder

4.3 Experimental Procedure

After selection of matrix material and reinforcements to be used the next important task was their casting. The flow chart of plan for fabrication and characterization of composites is shown below

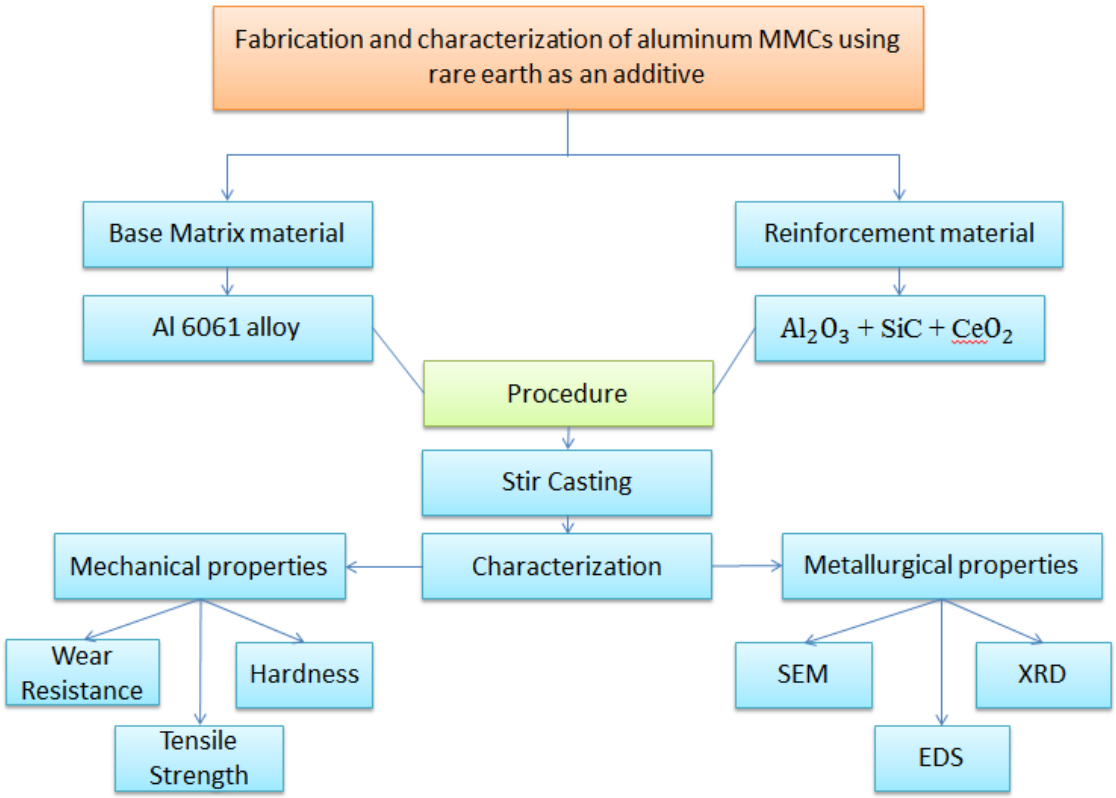

4.3.1 Fabrication of Al MMCs

Various techniques of fabrication of composites have been already discussed in chapter 1. It was observed that the processes such as powder metallurgy and diffusion bonding are very expensive as they need starting material which is very expensive such as powders or foil matrix etc. But as compared to solid phase processes, liquid phase process (casting process) is generally less expensive. The major challenge faced in the processing of liquid stir casting of MMCs was achieving a homogenous mixture of particulates, wettability and porosity and some undesirable chemical reactions. Distribution of particles was having a significant impact on the mechanical behavior of composites. Major components of stir casting setup includes: a graphite stirrer with reciprocating as well as rotational movement which is provides a homogenous distribution of particles in a molten alloy by stirring the melt at different speeds in order to achieve and to increase the wettability of particles, a lifting mechanism is used for stirrer assembly, a graphite crucible to hold the composition, argon gas supplier to prevent the composite from oxidation and to reduce overheating, bottom pouring unit and a die at the bottom. In a stir casting process (setup as shown in figure 5.2), the reinforcing phases, which are usually in powder form are distributed with the help of mechanical stirring into the molten aluminum. Before the mechanical stirring the surface of both should be properly cleaned so that the reaction between these two can be avoided. The particle distribution in the molten matrix also depends on the mechanical stirrer geometry, parameters of stirring, mechanical stirrer placement in the melt, melting temperature, and the characteristics of the particles added [12]. Sijo M T, K R Jayadevan [11] presents a study on analysis of stir cast aluminum silicon carbide metal matrix composite. A small description of various fabrication techniques was available in this study and stir casting route was considered as the simplest, cheaper and can be used for production on a mass level.

The schematic diagram of the setup used in this work is shown in fig 5.1.

- An amount of 900 grams of aluminum in the form of cubical blocks were been placed inside the graphite crucible and was been heated to a maximum temperature of 650°C to convert it into the molten form.
- The particulates of SiC and Al_2O_3 were mixed thoroughly and the packets of 5, 10, 15% of mixture were prepared which were then preheated in an muffle furnace (owen) for 1-2 hours at a temperature of 350-400°C to get their surface oxidized.

Figure 4.2 Muffle furnace (Courtesy: Foundry shop, PEC, Chandigarh)

- Similar process was been followed to prepare a mixture of (Al_2O_3+Sic + CeO_2) .
- The temperature required to heat up the aluminum alloy was taken as 650°C. Once the melt is prepared the reinforcements were added into the molten metal pool at a constant feed rate and was stirred continuously for about 8-10 minutes at a speed of 350 rpm with the help of graphite stirrer to get a homogeneous mixture of molten metal with the powder.

Figure 4.3 Stir casting setup (Courtesy: Foundry shop, PEC, Chandigarh)

- The molten metal mixture was then poured into a mold having three dies inside it i.e.

  a) Cylindrical shape of 220mm length and 25mm dia,
  b) Cylindrical shape of 220mm length and 20mm dia and
  c) one for impact specimen of cubical 10×10 mm shape.

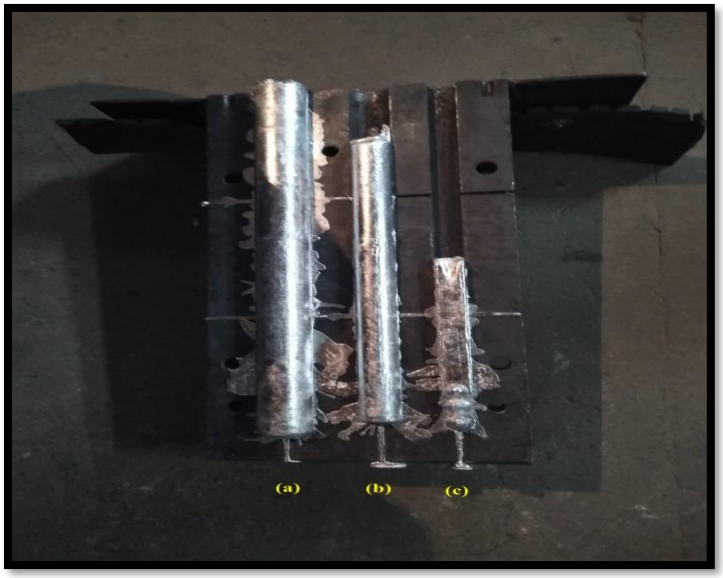

Figure 4.4 Cast iron die (Courtesy: PEC, Chandigarh)

The molten metal was allowed to be poured in all the three dies in equal proportion according to their shapes. The fabricated composite was allowed to solidify at room temperature and after solidification the samples were removed from the mold and were machined for further experimentation tests, the casted samples are shown in figure. All the 6 samples containing three samples of aluminum with reinforcement mixture of (SiC $+Al_2O_3$) and three samples with mixture of (Al_2O_3+Sic + CeO_2) were prepared by the same procedure.

4.3.2 Hardness testing machine

The hardness of the specimen was measured with the help of Vickers micro hardness tester and Rockwell hardness testing machine as shown in figure 5.4 and 5.5. Test samples must be prepared very carefully and properly by grinding and polishing. In Vickers micro hardness test procedure a diamond shaped indenter creates the indentation with a range of loads. By measuring the indentation with the help of Vernier scale

attached to it the hardness value is calculated. The indentation is allowed to be indented for 10-15 seconds and once it is over the two diagonal are measured and the required value is calculated. In this study the load applied was 5kg for duration of 10 seconds.

(a) (b)

Figure 4.5 (a) Vicker hardness tester (b) Rockwell Hardness tester (Courtesy: Solid mechanics lab, Thapar Institute of engineering & technology, Patiala)

The Rockwell hardness was measured on the Rockwell hardness tester with a load of 100kgf for the duration of 10 seconds. The indenter used in this test is a spherical shaped indenter. Once the indentation is completed the hardness value is indicated on the circular scale attached to the tester.

4.3.3 Scanning electron microscopy (SEM)

By using SEM the scanning of specimen is done with electrons of high-energy beam. When the electrons interact with the atoms present in the sample various signals are produced that contain information about the sample's surface topography and composition and various other properties. It can produce the specimen's surface images which are having very high-resolution, revealing less than one nano meter in size details.

Figure 4.6 Scanning electron microscopy (Make: JEOL JSM -6510LV, Oxford instruments) (Photo courtesy: SAI Labs, Patiala)

The specimen needed for the SEM should be conductive in nature as non-conductive specimens collect charge when scanned by the electron beam, which can cause faulty images. For non-conducting specimens, they are coated with ultrathin coating of electrically conducting material by either sputter coating or by high-vacuum evaporation. The specimens made for the SEM available at SAI Labs, Thapar technology campus, Patiala were 15×15 mm.

4.3.4 X-ray diffraction (XRD) machine

It is a most useful technique for qualitative and quantitative analysis of materials. It is basically used for identification of crystalline materials and analysis of unit cell dimensions. It consists of scattering of X-rays from the sample which interfere with each other either constructively or distructively. This means that the detectors can read-out signals only at angles where constructive interference occur.

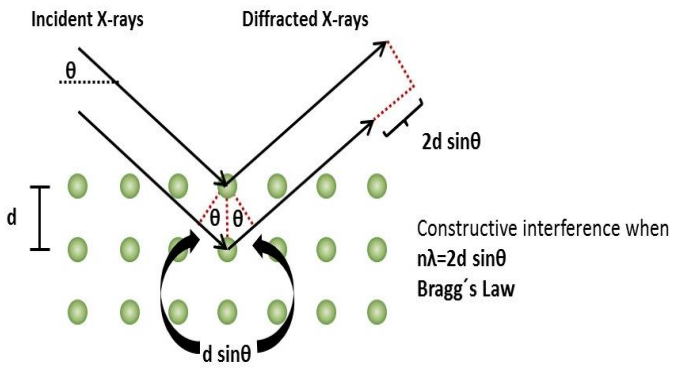

Figure 4.7 Schematic representation of Bragg's equation (Source: Wikipedia, https://wiki.anton-paar.com/en/x-ray-diffraction-xrd/##data-imagegroup-16856)

X-ray diffraction shows unique fingerprints associated with the crystal structure. It is a non-destructive analytical technique.

Figure 4.8 X-ray diffractometer (Photo courtesy: SAI labs, Patiala)

4.3.5 Wear testing (Pin-on-disc tribometer)

A pin on disc tribometer (Ducom India) is used to calculate dry wear characteristics of the composites. It consists of a stationary pin that is normally loaded against a rotating disc. The pin can be in any shape according to the test. Wear specimens made for the test were of cylindrical shape with diameter 10 mm and length 12 mm and were clamped in the square clamp (V-shaped) against the rotating disc of 160 mm diameter. The rotating disc was of EN31 steel material. Acetone was used to clean the disc as well as specimens before starting the experiment.

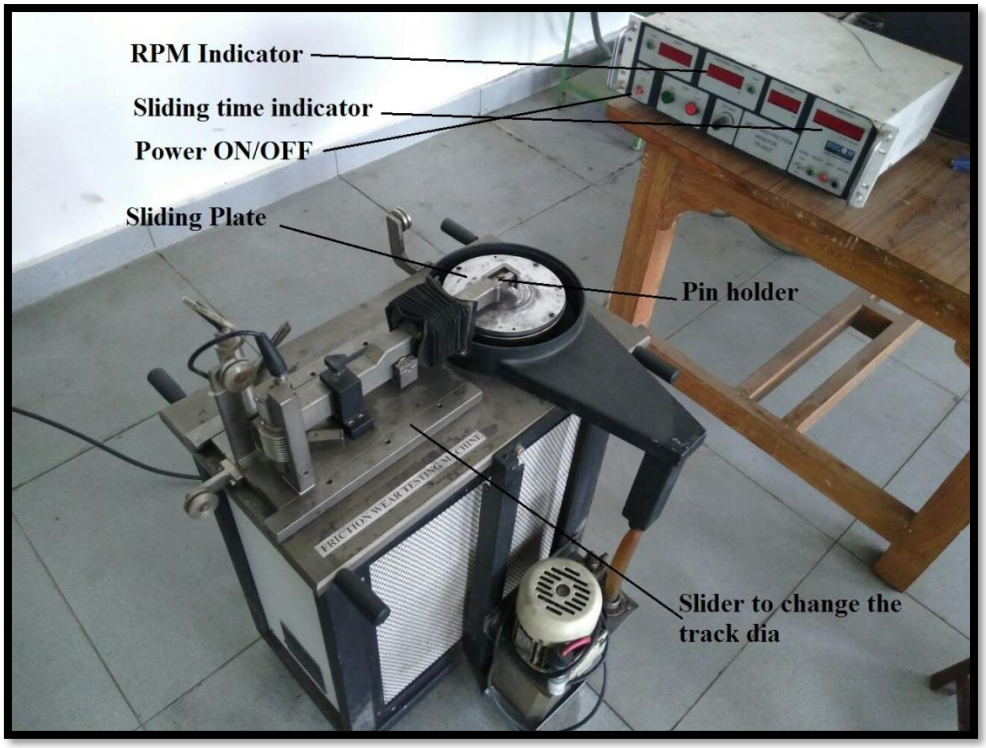

Figure 4.9 Wear testing machine (Pin-on-disc tribometer) (Photo courtesy: Machine tool lab, TIET, Patiala)

The details consisting of various sliding parameters used for the completion of the objectives of the current work is shown in table 5.1.

Table 4.4 Details of sliding wear parameters

PARAMETERS	**DESCRIPTION**
Testing specimens and samples	Pin-on-disc (a) Al 6061 alloy + Al_2O_3 + Sic (b) Al 6061 alloy + Al_2O_3 + Sic + CeO_2
Counter disc	Material of disc = EN 31 Steel Hardness of disc = 105 HRB Diameter of disc = 160 mm
Sliding distance (m)	500, 1000, 1500, 2000
Sliding Velocity (m/sec)	0.5, 1, 2
Normal loads (N)	10, 20, 30
Lubrication Condition	Dry condition
Temperature (°C)	Atmospheric temperature

4.3.6 Universal testing machine (UTM)

A UTM machine is used to measure tensile strength and compressive strength of the materials. The universal part of the name means it can perform many standard tensile and compressive tests on materials, components and structures. After the test is completed the output is shown on a digital screen where the results are in the form various graphs i.e. stress vs strain and load vs displacement. With the help of these graphs various values like yield strength, %age elongation, ultimate tensile strength (UTS) etc. can be obtained. The Universal testing machine used in this work has the following specifications

Table 4.5 Details of UTM machine used

Instrument Used	**UTE 100**
Make	Fuel instruments & engineering pvt. Ltd. (FIE)
Capacity	1000 kN
Resolution	0.05 kN
Temperature	25±3ºC

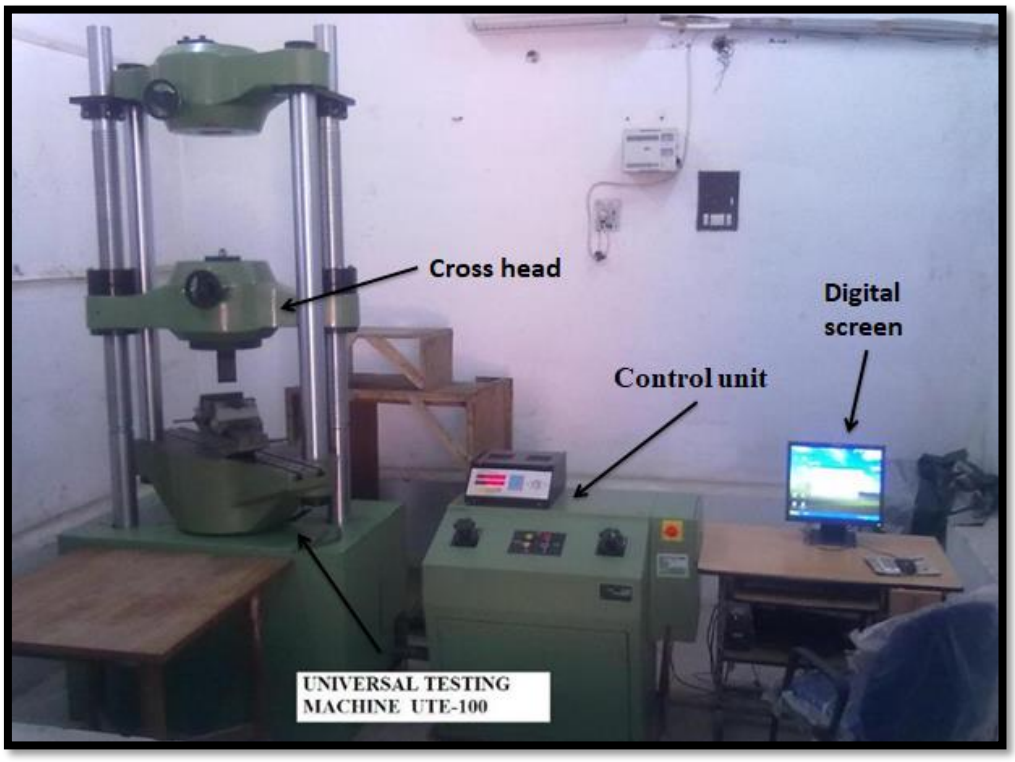

Figure 4.10 Universal testing machine (UTE100) (Photo courtesy: CITCO-IDFC testing laboratory, Chandigarh)

Chapter 5

Results and discussions

5.1 Introduction

Composites of Al 6061 alloy + Al_2O_3 + Sic as well as Al 6061 alloy + Al_2O_3 + Sic + CeO_2 were successfully fabricated using stir casting technique. The following sections describe the characterization of the composites.

5.2 MICROSTRUCTURE ANALYSIS

The basic aim behind this philosophy of producing hybrid composites is to see the effect of rare earth oxides mainly CeO_2 on the properties and microstructure of Al6061 alloy. The preheated rare oxide reinforcement in powder form is mix into the liquid-aluminum alloy to produce the hybridization effect into the composites. Throughout the experimental process different sizes of CeO_2 rare earth oxides, SiC and Al_2O_3 particles mixed with the aluminum alloy matrix to form hybrid composites. After the proper mixing, Al_3Ce, Al_4Ce, $CeAl_{11}O_{18}$, high porous alpha alumina and SiC particulate in uniform form has obtained in the form of cake.

5.2.1 SEM analysis of hybrid composites

From SEM images of various percent compositions of Al_2O_3 and SiC based hybrid composites, the pattern of microstructure Al_2O_3 particles seems to be very fine as compared to the particle pattern of the SiC. Because of the flaky shape of the Al_2O_3 particles, it is very difficult to pull out these Al_2O_3 particles as compared to the SiC particles of irregular shape results in the improvement in the tensile properties of the hybrid composites (Altinkok 2004) (35). The microstructure of Al_2O_3/SiC reinforcement based hybrid composites is shown in Fig 6.15 (a), (b) and (c) with various percent of SiC and Al_2O_3, so that total percentage of reinforcement could not reach above 30%. From the electron image of microstructure, the aluminum phase invade into the ceramic cake uniformly results into the more improved composites. Aluminum phase has also intruded into the open pores of the struts as seen in the electron image of the composites. As the grain of alumina grows in size, the preform obtained looks like a honey comb structure which finally results in the successful reinforcement of alumina matrix (Altinkok 2004)

(35). Because of the uniform distribution of Al_2O_3 and SiC particle into the matrix of Al6061 alloy leads to the better tensile properties.

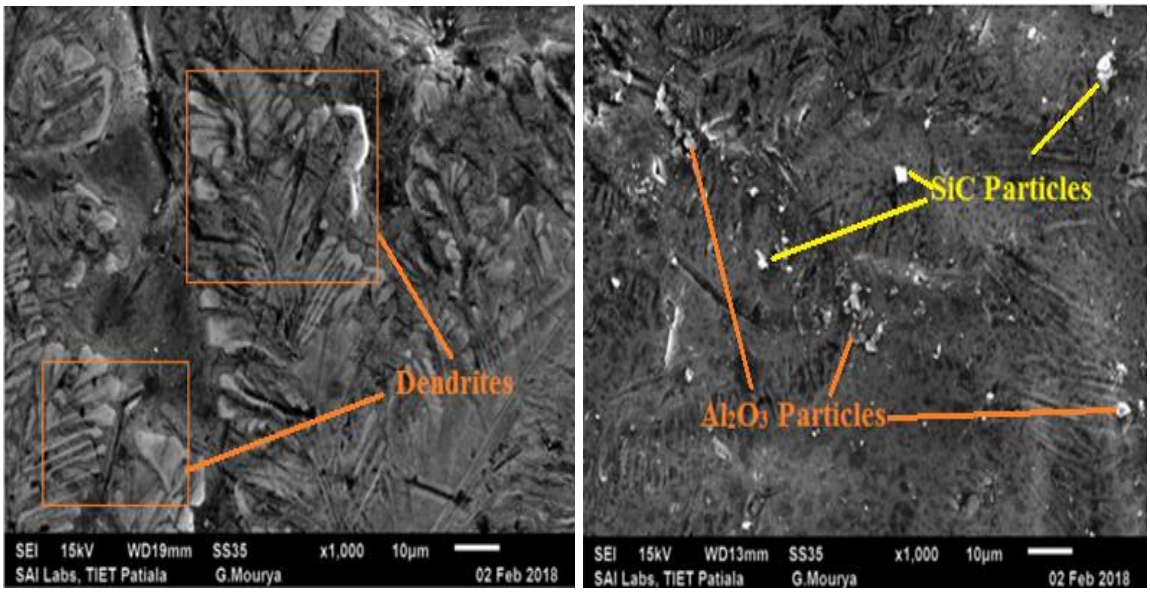

(a) (b)

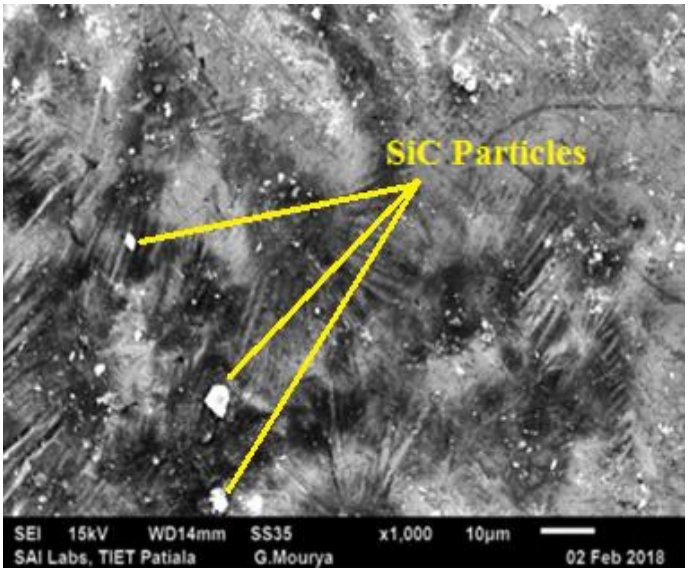

(c)

Figure 5.1 SEM microstructure images of (a) Al6061 + 2.5% Al_2O_3 and 2.5% SiC (b) Al6061 + 5% Al_2O_3 and 5% SiC (c) Al6061 + 7. 5% Al_2O_3 and 7.5% SiC

Very fine and smooth structure of hybrid composites seen using rare earth oxides as reinforcement element. From the SEM images of hybrid composites it was seen that degree of agglomeration reduces which results of the smoothened surface achieved after stir casting. The powder form of CeO_2 nano- oxides reacts with the aluminum matrix form a uniformly dispersed phase. As the composites made of Al_2O_3 and SiC reinforcement

lacks in the better performances perspective. Certain amount of rare earth oxides add into them to improve its tensile properties and enhance the ductility of the components which makes them suitable for the aerospace application. Several Researchers have been reported that addition of cerium oxide (CeO_2) as a rare earth metal refines as well as there is a transformation in the microstructure of hypereutectic Al_2O_3-SiC alloy by changing the morphology of eutectic silicon from plate like acicular structure to fibrous one (Tsai et al. 2011) (36) . Rare earth compounds can be better choice to act as a nucleation site for the silicon, if they are able to solidify at higher temperature than the silicon although having the same crystal structure as that of Silicon. However it was found that cerium react with aluminum to form AlCe orthorhombic compound which has a melting point of 845^{o}C.The crystal structure of cerium oxide is very much different from the Si, that's why the CeO_2 could not be better choice to behave as nucleants for the refinement of the primary Si particle, even though the cerium compound solidifies at a higher temperature than Si. Thus, to fulfill the condition of heterogeneous nucleation its path of mechanism of refinement of primary silicon and eutectic silicon cannot attribute to it. of primary silicon refinement mechanism particles in hypereutectic Al_2O_3-SiC alloy reinforced with the cerium oxide should be based on the decrement in nucleation temperature of Si and modification of both solid-liquid interfacial energy and also related to the surface energy of solid silicon. Moreover the improvement in the chemical composition of the molten alloy and fragmentation of various solidifying constituent can be achieved by the proper stirring in the stir casting by reinforcing CeO_2 which ultimately lead to the refinement of both primary Si and eutectic Si. Cerium oxide particulate helps in matrix grain refinement as clearly mentioned in the microstuctural view as compared to the without rare microstructure of matrix

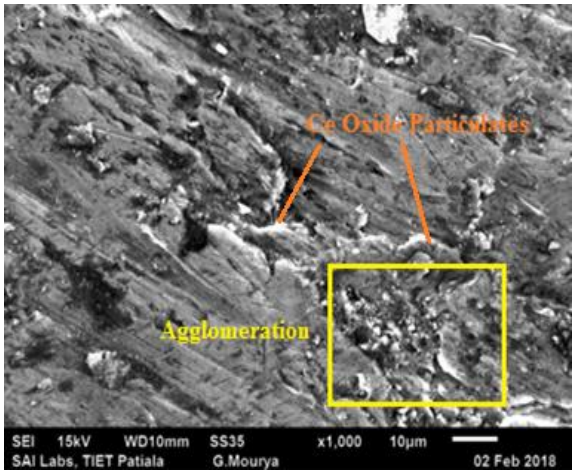

(a)

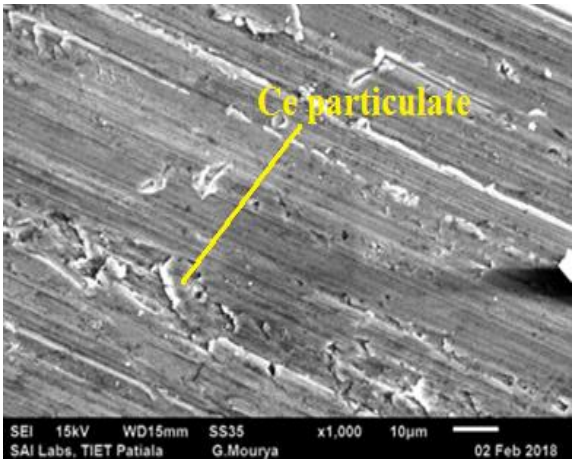

(b)

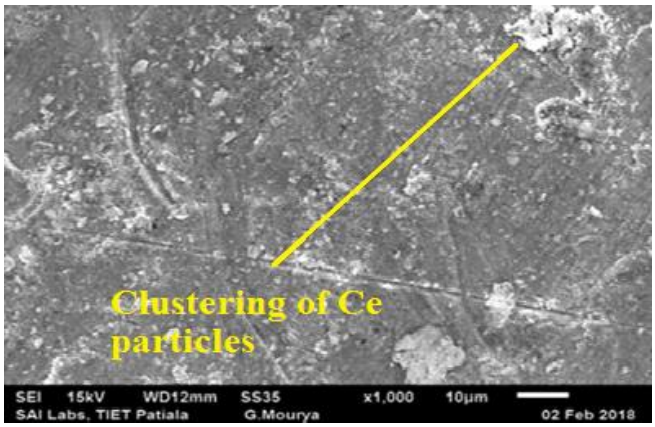

(c)

Figure 5.2 SEM images of (a) Al6061 + 2. 5% Al_2O_3 and 2.5% SiC ceramic with 0.5% CeO_2 (b) Al6061 + 5% Al_2O_3 and 5% SiC ceramic with 1.5% CeO_2 (c) Al6061 + 7.5% Al_2O_3 and 7.5% SiC ceramic with 2.5% CeO_2

5.2.2 X-ray diffraction analysis of various phases of hybrid Composites

X-ray diffraction is an important technique to understand the properties of hybrid composites based on various powder mix elements like CeO_2, Al_2O_3 and SiC prepared by the stir casting technique. Each plot of XRD indicates the characteristics of the hybrid composites samples consists of various percent composition of powder mix reinforcement elements. In each case the 2θ value varies from 20^o to 110^o. In most of the cases, the highest peak was observed on 2θ at 38 values as indicated in each case. The various patterns of different composition of Al_2O_3 and SiC powder based reinforcement hybrid composites as shown in Fig 5.3. As the parent material mainly consists of aluminium in matrix form due to which the large peaks corresponds to the parent metal. XRD analysis also reveals that the smaller peaks corresponds to the presence of various phases like SiO_2,$Mg(CO_3)$,$FeAl_2Si$ in hybrid composites. The various patterns of different composition of CeO_2, Al_2O_3 and SiC powder based reinforcement hybrid composites as shown in Fig 5.3. The XRD study of modified CeO_2 - aluminium alloy showed that presence of Al, SiO_2, Mg_5Si_6, MgO, Ce_2O_3 and $Ce_{11}O_{20}$ phases . The presence of Ce_2O_3 and $Ce_{11}O_{20}$ indicated cerium oxide has been successfully added as a rare earth oxides in the aluminium alloy Al-6061.

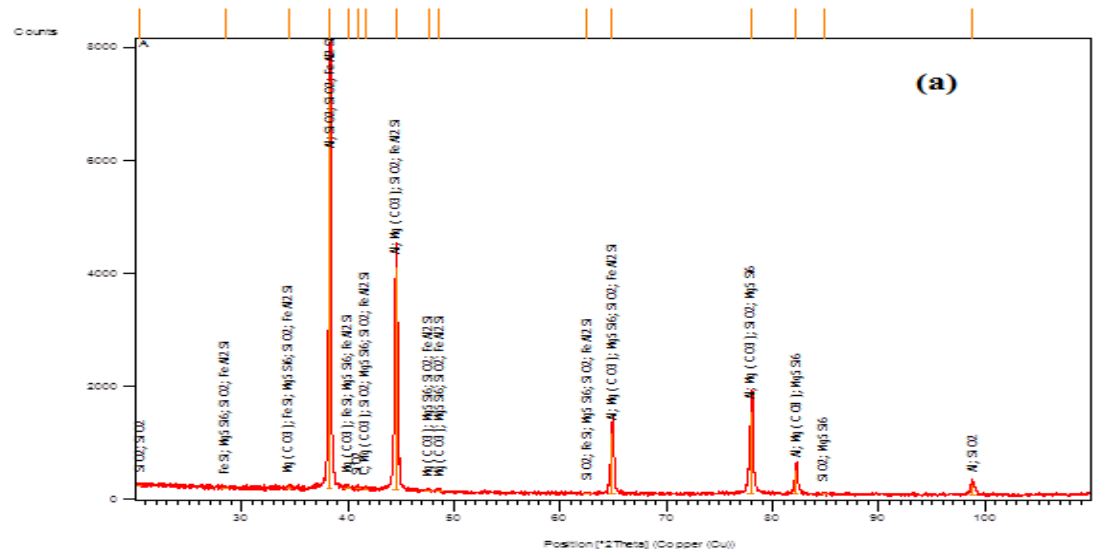
Counts
(a)
Position [°2Theta] (Copper (Cu))

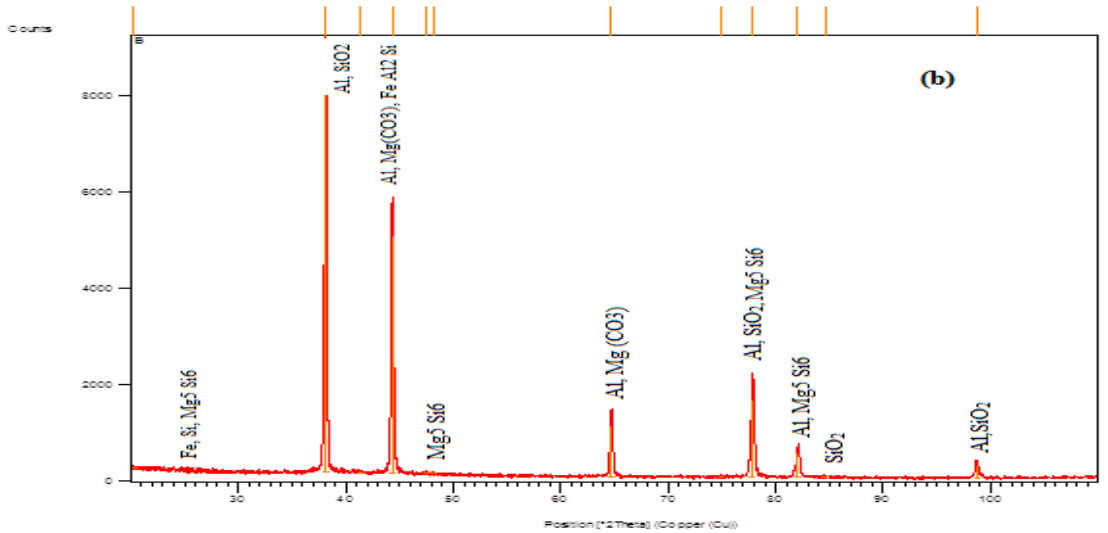
Counts
(b)
Al, SiO2
Al, Mg(CO3), Fe Al2 Si
Fe, Si, Mg5 Si6
Mg5 Si6
Al, Mg (CO3)
Al, SiO2, Mg5 Si6
Al, Mg5 Si6
SiO2
AlSiO2
Position [°2Theta] (Copper (Cu))

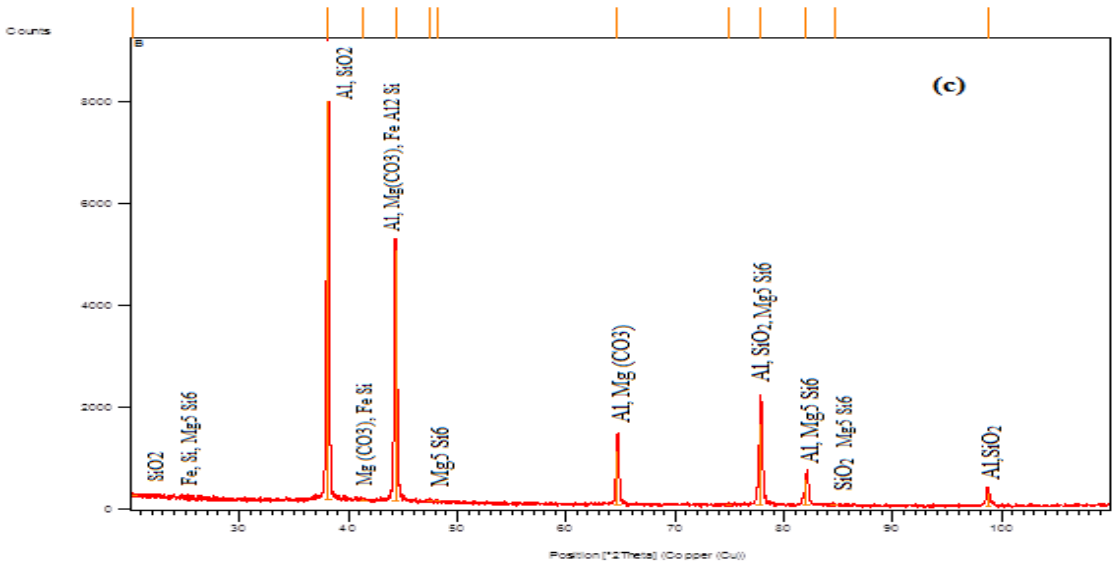
Counts
(c)
Al, SiO2
Al, Mg(CO3), Fe Al2 Si
SiO2
Fe, Si, Mg5 Si6
Mg (CO3), Fe Si
Mg5 Si6
Al, Mg (CO3)
Al, SiO2, Mg5 Si6
Al, Mg5 Si6
SiO2 Mg5 Si6
AlSiO2
Position [°2Theta] (Copper (Cu))

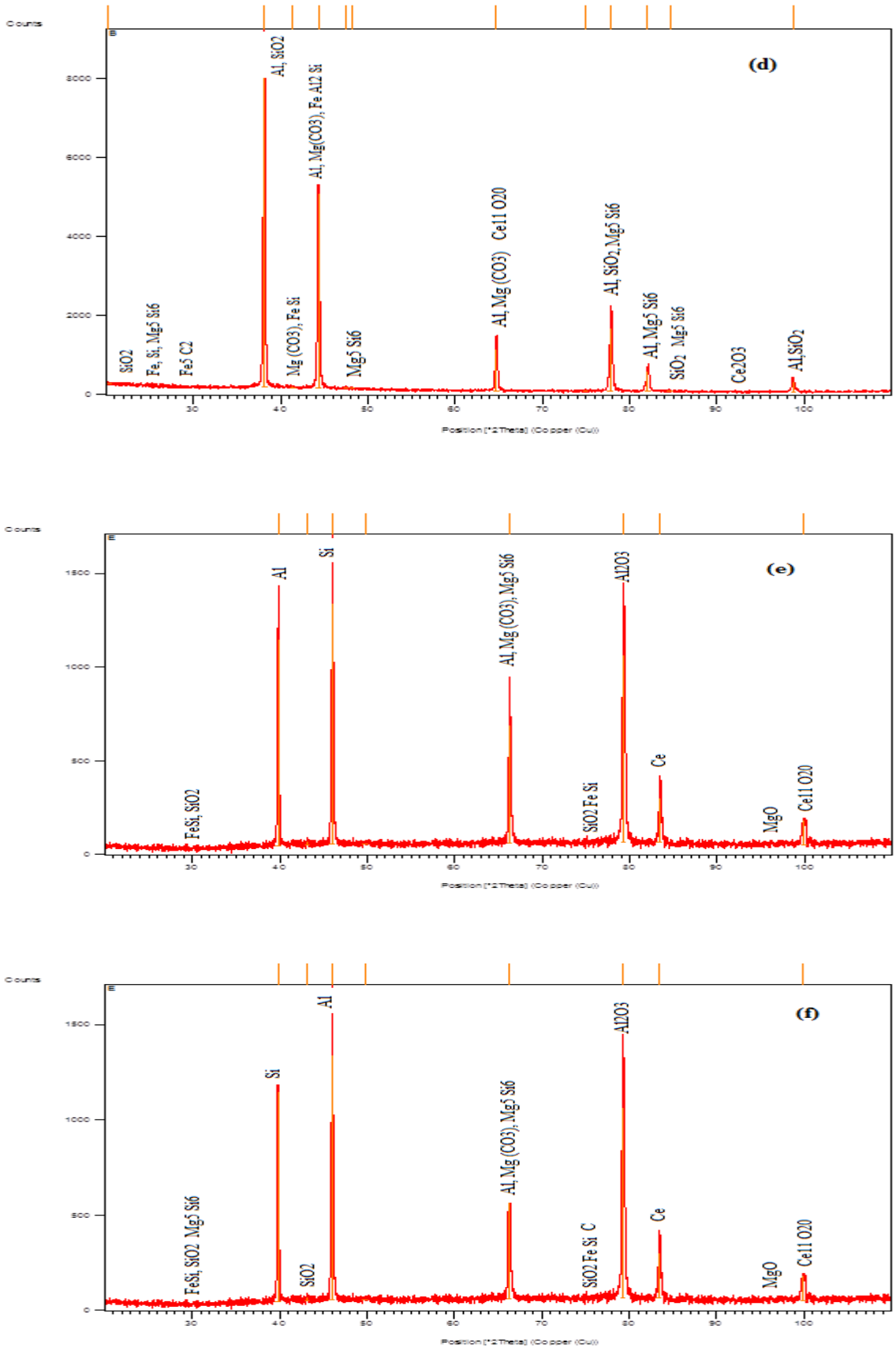

Figure 5.3 XRD images of (a) 5% (Al_2O_3 + SiC) without rare (b) 10% (Al_2O_3 + SiC) without rare (c) 15% (Al_2O_3 + SiC) without rare (d) 5% (Al_2O_3 + SiC) with 0.5% CeO_2 (e) 10% (Al_2O_3 + SiC) with 1.5% CeO_2 (f) 15% (Al_2O_3 + SiC) with 2.5% CeO_2

5.2.3 EDS Analysis

Energy dispersive spectroscopy analysis of the Al_2O_3/SiC/CeO_2 – reinforced composites is shown in Fig 5.4 (a) to Fig 5.4 (f). It is clear from the spectroscopy analysis that oxygen and carbon peaks were observed. It is very much confirms from the EDS analysis that aluminum SiC particles and cerium oxide are present within the composites. Therefore, these results of SEM indicated that successful incorporation of Hybrid ceramics Al_2O_3/SiC/CeO_2-reinforced Al-matrix composites produced by the stir casting process.

Fig 5.4 (b), (d) and (e) shows the EDS images of the hybrid composites with 0.5%,1.5% and 2.5% of cerium oxide as weight percent. The EDS results of selected area of indicated as spectrum 2 in every case with rare earth powders suggests that good metallurgical bonding between the hybrid oxides (Al_2O_3/SiC) and CeO_2 with Al6061matrix were achieved in the hybrid composites. The higher magnification of interface images indicates that the interface was very much smooth and clear, which further indicated that at interface no reaction has been occurred. It is well acknowledged that in the system composed of hybrid ceramic Al/SiC there may be a tendency for the development of the hazardous product Al_4C_3 at the interface of Al/SiC from the dissolution of SiC by liquid aluminum during reaction. However, the formation of Al_4C_3 can be retarded by the selection of proper processing temperature and duration time during stir casting process. In this study, the preheating of the Al/SiC/CeO_2 was done at the temperature of 383^{o}C in the furnace at least for 60min and then slowly put into the molten Al6061 matrix at temperature upto 850^{o}C simultaneously with stirring 15 to 20 minutes. At these suggested parameters, formation of Al_4C_3 has been stopped after the reaction between SiC particles and the Al matrix. Furthermore, it has been demonstrate that silicon can be act as a catalytic inhibitor which greatly helps in the potential attack of SiC reinforcement by liquid aluminum at the Al/SiC interface. Such things can be beneficial for obtaining good mechanical properties.

From various SEM images of the hybrid composites with different contents of CeO_2 nanoparticulate powders, it was clear that the CeO_2 nanoparticulate tended to be located at grain boundaries and form clusters around these grains. These cluster formation may influence the mechanical properties of the hybrid composites. With the addition of nanoparticulate cerium oxide, the average grain size of the hybrid composites decreased. This indicated that the introduction of CeO_2 nanoparticles into the Al6061 matrix can facilitate the refinement of the structured composite. This effect of grain refinement called as Zener – Hollomon pinning which stated that the pinning effect of the small second-phase particles on the grain boundaries. The CeO_2 nanoparticles which were present at the junction of the three grains can slow down the growth of grains by pinning the grain boundaries. Because of the thermal mismatch between Al6061 matrix and CeO_2 reinforcement's leads to the dislocations and the dislocation density followed an increasing trend with increase in CeO_2 contents. These two effects combined together helps in the enhancement of the strength of the hybrid composites.

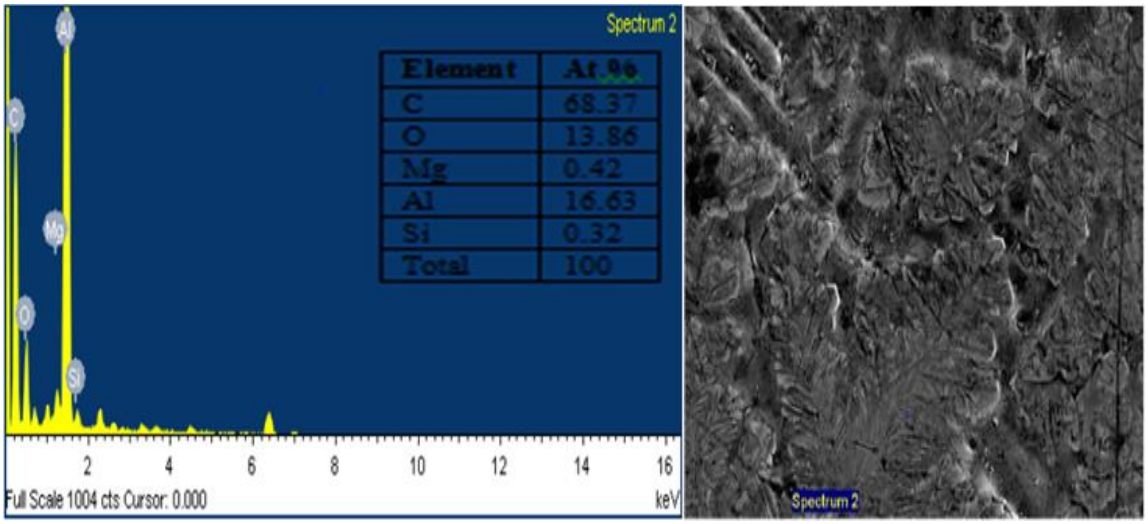

(a)

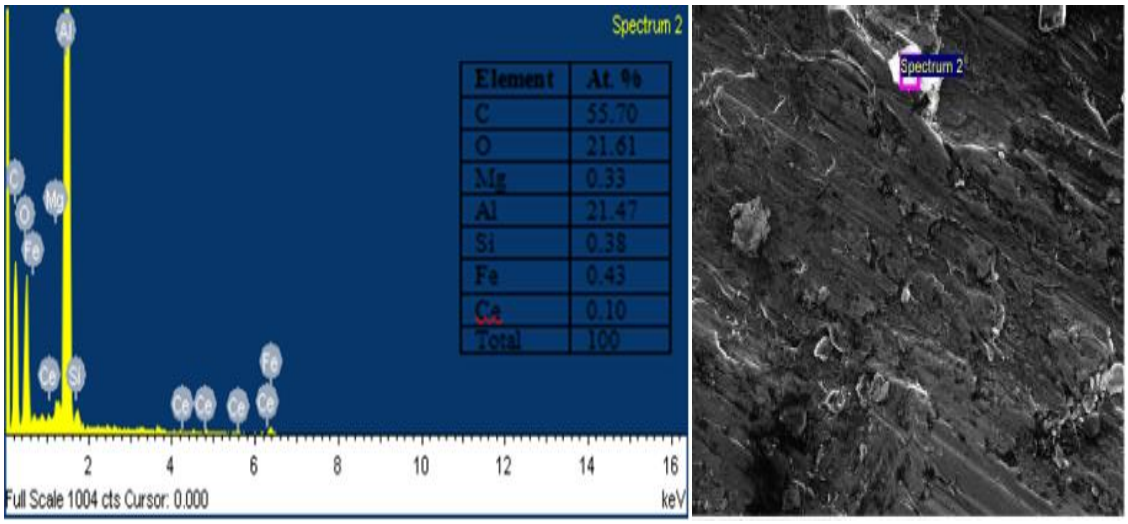
Spectrum 2
Element At. %
C 55.70
O 21.61
Mg 0.33
Al 21.47
Si 0.38
Fe 0.43
Ce 0.10
Total 100
Full Scale 1004 cts Cursor: 0.000
keV
Spectrum 2

(b)

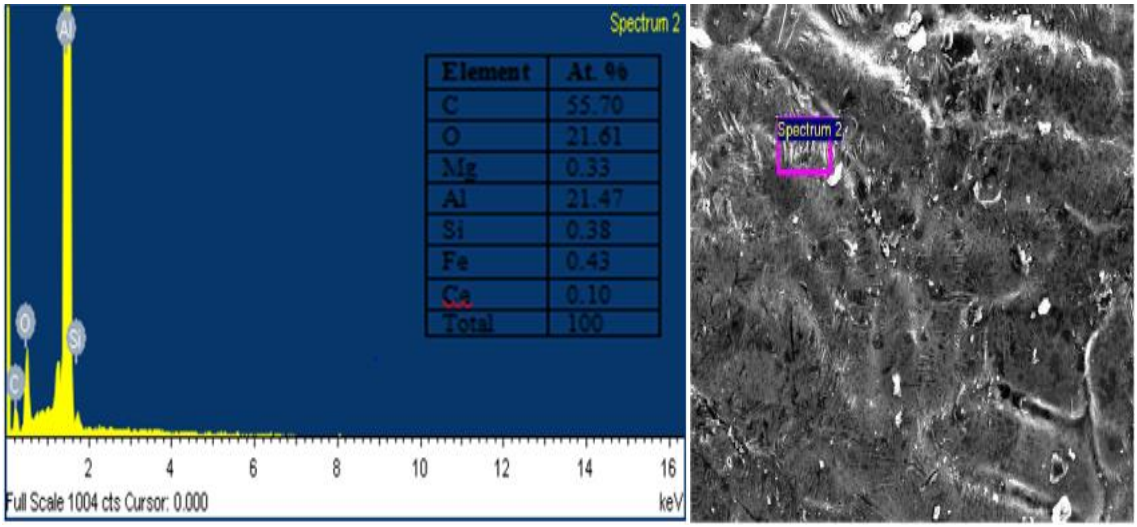
Spectrum 2
Element At. %
C 55.70
O 21.61
Mg 0.33
Al 21.47
Si 0.38
Fe 0.43
Ce 0.10
Total 100
Full Scale 1004 cts Cursor: 0.000
keV
Spectrum 2

(c)

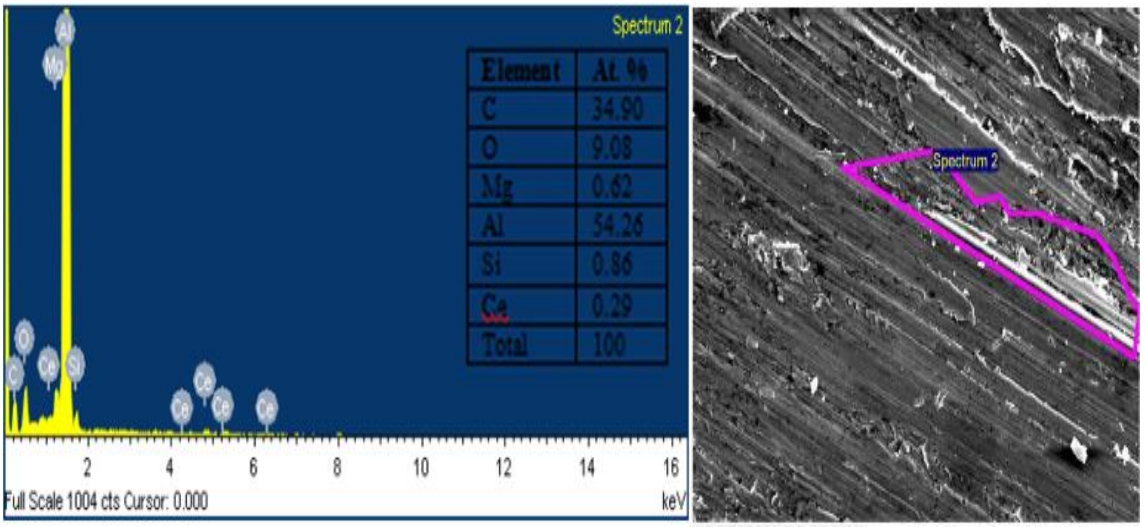
Spectrum 2
Element At. %
C 34.90
O 9.08
Mg 0.62
Al 54.26
Si 0.86
Ce 0.29
Total 100
Full Scale 1004 cts Cursor: 0.000
keV
Spectrum 2

(d)

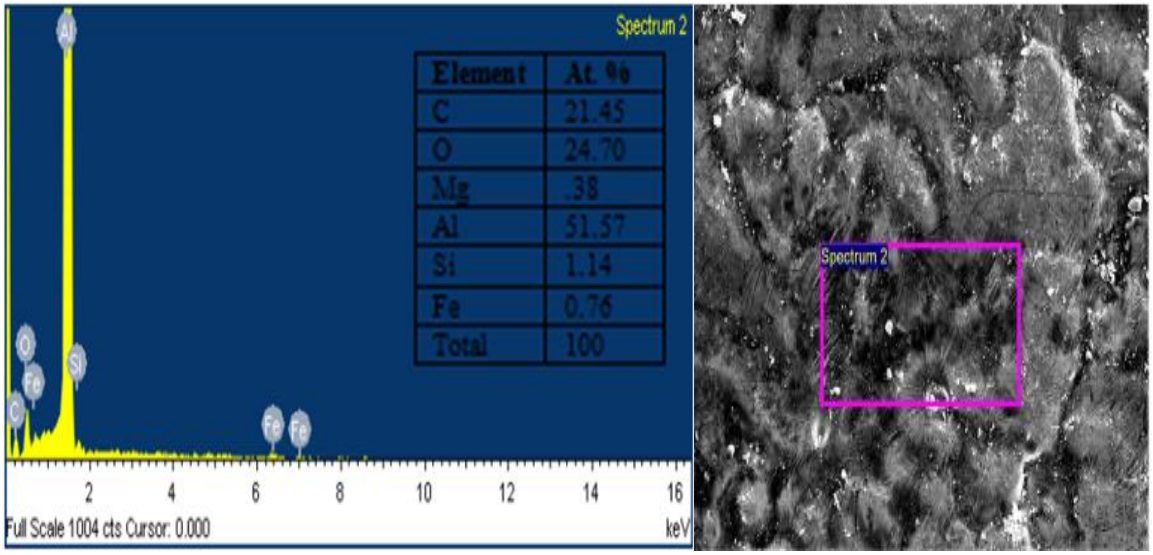

(e)

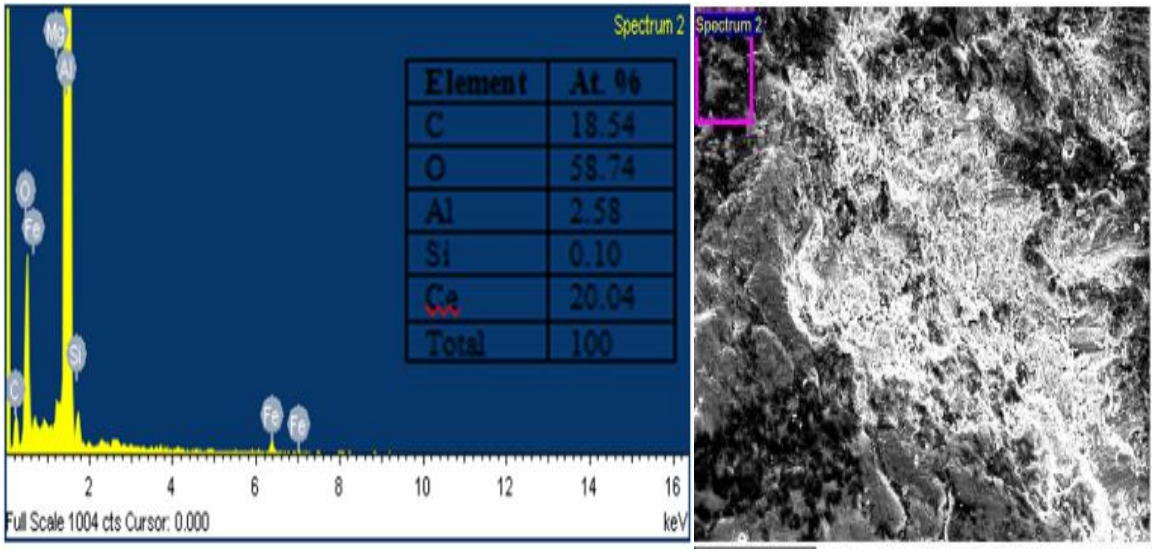

(f)

Fig 5.4 EDS analysis of Hybrid composites, a) 2.5% Al_2O_3 + 2.5% SiC without rare, b) 0.5 % CeO_2 with rare,c) 5% Al_2O_3 + 5% SiC without rare, d) 1.5 % CeO_2 with rare, e) 7. 5% Al_2O_3 + 7.5% SiC without rare and f) 2.5 % CeO_2 with rare

5.3 HARDNESS STUDY

5.3.1 Vicker Hardness testing (Micro hardness study)

The hardness of the base metal alloy Al-6061 and hybrid composite samples are reported in table 6.1. The test reveals that the value of hardness of hybrid composites with rare earth material as an additive is higher in comparison to the composites with no rare earth addition. It can be seen that when the rare earth element content is 0.5% the hardness

value increases a little and when the composition reaches 1.5% there was a slight increase in values but when the composition reaches 2.5% there was a sudden increase in the hardness value as compared to the base alloy and non- rare earth composites. Also it can be seen that with increase in reinforcement in both the cases (Al_2O_3+Sic + CeO_2 as well as Al_2O_3+SiC) composites there is an increase in the hardness values. This can be because with the increase in amount of reinforcement the density of the material also increases which tends to harden the matrix and hence hardness of the material increases.. The Vicker's hardness value of the base alloy was increased by 33 % by addition of 2.5% rare earth along with (Al_2O_3+Sic) mixture and as compared to non-rare earth element (Alloy+ 15%(Al_2O_3+ Sic) mixture the hardness increased by 15.04%.

Table 5.1 Vicker hardness values of composites.

SAMPLES	**HV 1**	**HV 2**	**HV 3**	**HV Average**
Al alloy	80	79	79	79.3
Alloy+ 5%(Al_2O_3+ Sic)	85	85	84.5	84.8
Alloy+ 10%(Al_2O_3+ Sic)	85	85.5	86	85.5
Alloy+ 15%(Al_2O_3+ Sic)	91	89.5	90	90.17
RARE EARTH COMPOSITES				
Alloy+ 5%(Al_2O_3+ Sic) + 0.5% CeO_2(Rare earth)	85	87	85	85.67
Alloy+ 10%(Al_2O_3+ Sic) + 1.5% CeO_2(Rare earth)	88	88	88.5	88.17
Alloy+ 15%(Al_2O_3+ Sic) + 2.5% CeO_2(Rare earth)	92	92.5	94	92.8

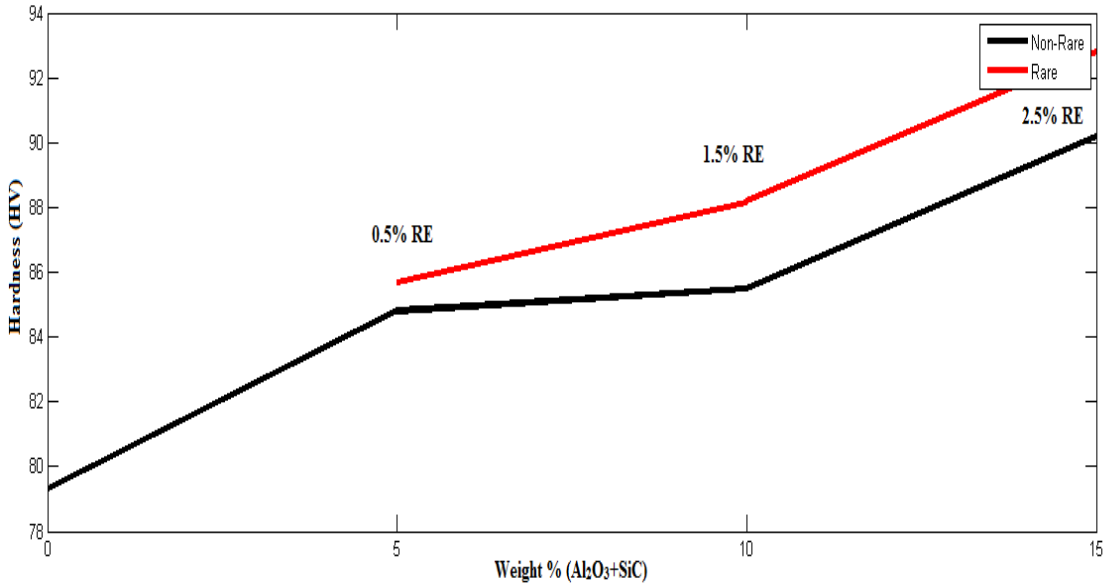

Figure 5.5 Micro- Hardness distribution for Non-rare earth and rare earth composites

5.3.2 Rockwell Hardness testing

The Rockwell hardness test was performed under 100 kgf loads. The following are the values of the hardness under Rockwell scale. The graphical representation of the hardness values are shown below

Table 5.2 Rockwell hardness values of composites.

SAMPLES	HRB 1	HRB 2	HRB 3	HRB Average
Al alloy	61.6	61.3	62.3	61.73
Alloy+ 5%(Al_2O_3+ Sic)	62.6	61.9	62.6	62.37
Alloy+ 10%(Al_2O_3+ Sic)	67.0	66.6	67.4	67
Alloy+ 15%(Al_2O_3+ Sic)	72.0	72.0	71.6	71.8
RARE EARTH COMPOSITES				
Alloy+ 5%(Al_2O_3+ Sic) + 0.5% CeO_2(Rare earth)	72.4	72.8	72.8	72.67
Alloy+ 10%(Al_2O_3+ Sic) + 1.5% CeO_2(Rare earth)	72.86	72.8	72.8	72.82
Alloy+ 15%(Al_2O_3+ Sic) + 2.5% CeO_2(Rare earth)	82.6	83.1	82.1	82.6

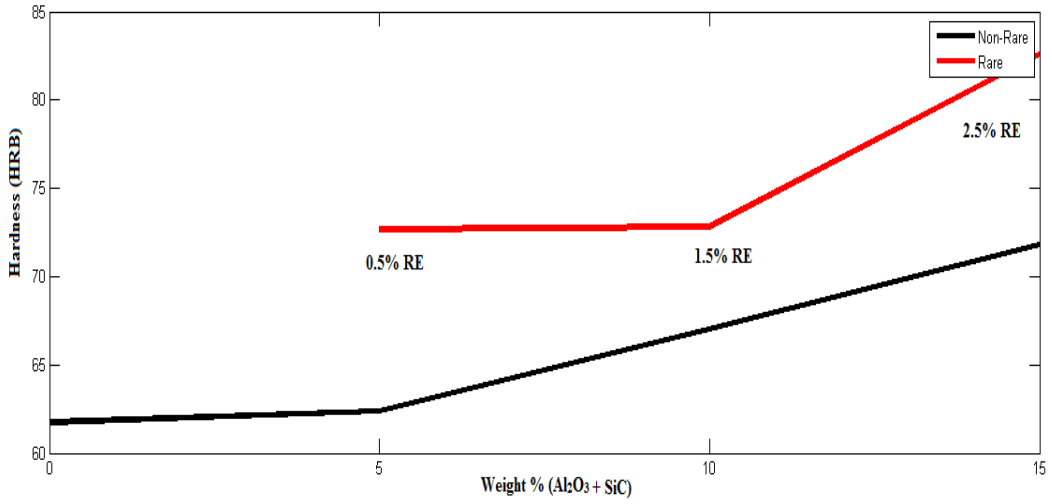

Figure 5.6 Rockwell hardness distributions for Non-rare earth and rare earth composites

5.4 Wear test

The wear test was performed on pin-on-disc tribometer. It was performed for only two samples. The samples were selected according to the value of maximum hardness from both the cases i.e composite of Alloy+ 15% (Al_2O_3+ Sic) mixture and Alloy+ 15% (Al_2O_3+ Sic) + 3% CeO_2 (Rare earth). These two composites having maximum hardness from both the groups i.e. non-rare earth composite and rare earth composites were selected to further perform the wear test.

Cylindrical pin specimens of dia 10mm and length 12mm were machined from the base alloy and hybrid composite of Al_2O_3+Sic mixture and composites with Al_2O_3+Sic + CeO_2 mixture. Dry sliding wear test was been carried out on PIN-ON-DISC TRIBOMETER. Before starting the wear test all the specimens for test were finished and grinded using emery paper of varying grades. All wear test were conducted at three different sliding velocities i.e. 0.5 m/sec, 1 m/sec, 2 m/sec under three normal loads values i.e. 10 N, 20 N, 30 N. The weared out specimens were then tested under SEM to check cracks and other effects of wear test. Progressive wear was calculated at different sliding distances i.e. 500m, 1000m, 1500m, and 2000m at different sliding velocities.

5.4.1 Effect of sliding velocity

Figure 6.3 represents the effect of wear rate w.r.t. sliding velocity and it can be seen that as the sliding velocity increases from 0.5 to 2 m/sec there is a decrement in the wear rate. A thinner and less adherent lubricant layers peels off from the surface when the sliding velocity increases, forming a layer of oxide which prevents the composite specimen from further volume loss. Further increase in sliding speed reduces the contact time between

the pin and the disc which further results in decrement of wear loss. As it can be seen from the graph the values of wear loss decreases with increase in the sliding velocity in all the cases, but there are few cases where there is an increase in wear loss from velocity range of 1 to 2 m/sec i.e. for composite with mixture of Al_2O_3+Sic + CeO_2 at 30 N load, Al_2O_3+Sic at 20 N load and al alloy 6061 at 20 N load. Therefore EDS analysis of the wear debris of these composite specimens were done and it was revealed that a small amount of iron particles were present which were not found in any of the other cases. The presence of iron particles on the surface makes an iron rich layer over the surface can be the reason for the slight increase in the value of wear loss of the mentioned specimens.

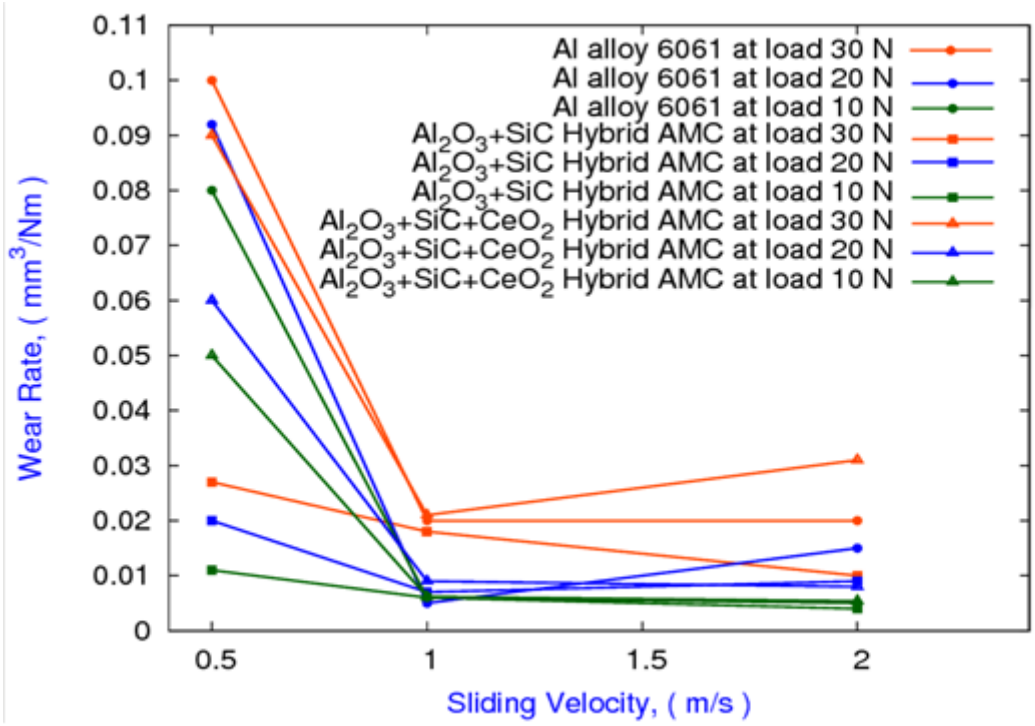

Figure 5.7 Graphical representation of wear rate vs. sliding velocity

5.4.2 Effect of applied load

The wear rate plots for Al-alloy 6061, composite of Al_2O_3+Sic mixture and with Al_2O_3+Sic + CeO_2 mixture were plotted against normal load and different sliding velocities in fig. The obtained wear rates for all the parts are shown in fig. It can be seen from the figure that the composite with Al_2O_3+Sic + CeO_2 mixture has shows better wear resistance throughout the range of parameters. It can be observed from the figure that the wear rate increases with the increase in normal load. The wear rate of base Al-alloy 6061

was more as compared to other two composites. As it can be seen from the steady-state wear equation that

$$V = K\frac{PL}{3H}$$

Where,

V represents volumetric loss, H is the hardness value HV, P is the normal load, L is the sliding distance and k is the dimensionless standard wear constant.

As the hardness of the composite with Al_2O_3+Sic + CeO_2 mixture is more as compared to the composite of Al_2O_3+Sic mixture therefore the wear resistance will also be more and it can be seen in fig. And also the maximum wear rate was found at higher value of load and decreases with decrease in the value of normal load.

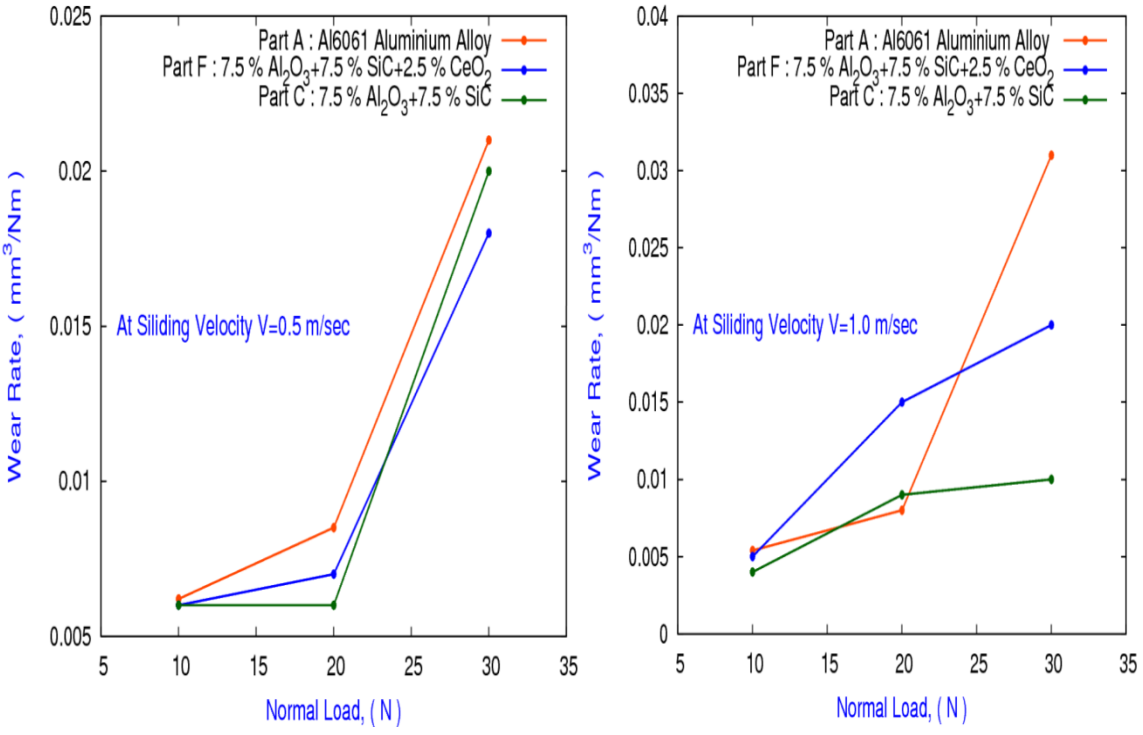

(a) (b)

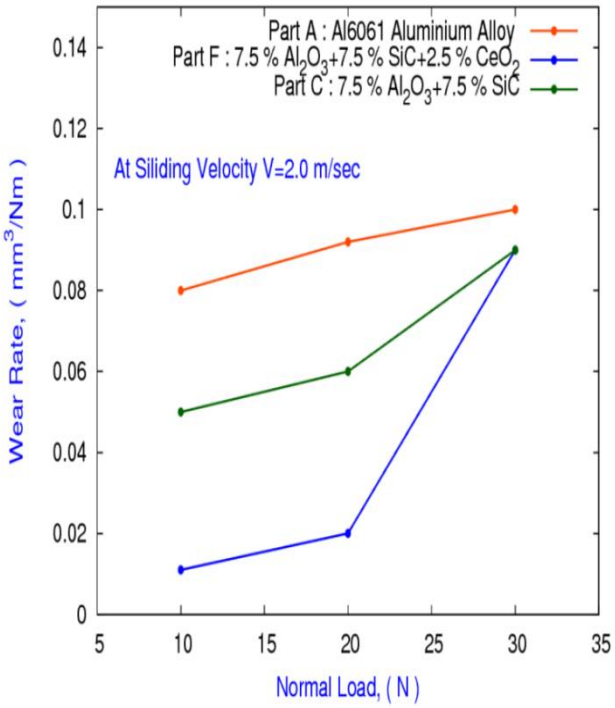

(c)

Figure 5.8 Graphical representation of cumulative weight loss at (a) 0.5m/sec (b) 1m/sec (c) 2m/sec sliding velocities

5.4.3 Effect of sliding distance

The wear specimens were tested for different sliding distances at different sliding velocities to check the progressive wear rate of the samples after certain distance and time. It was observed that during the initial stage i.e. run-in period the wear rate becomes very high because it is the primary stage of wear and at this stage surfaces adapt to each other and maximum wear rate can be observed in this stage. Once this stage is crossed the next sage that comes into picture is secondary stage or mid-age process in which the wear tends to reduce and further remains constant. Steady wear is observed under this stage. Most of the components operational life is spent in this stage. The various stages undergone by the composite specimens are shown through a graphical representation as shown below.

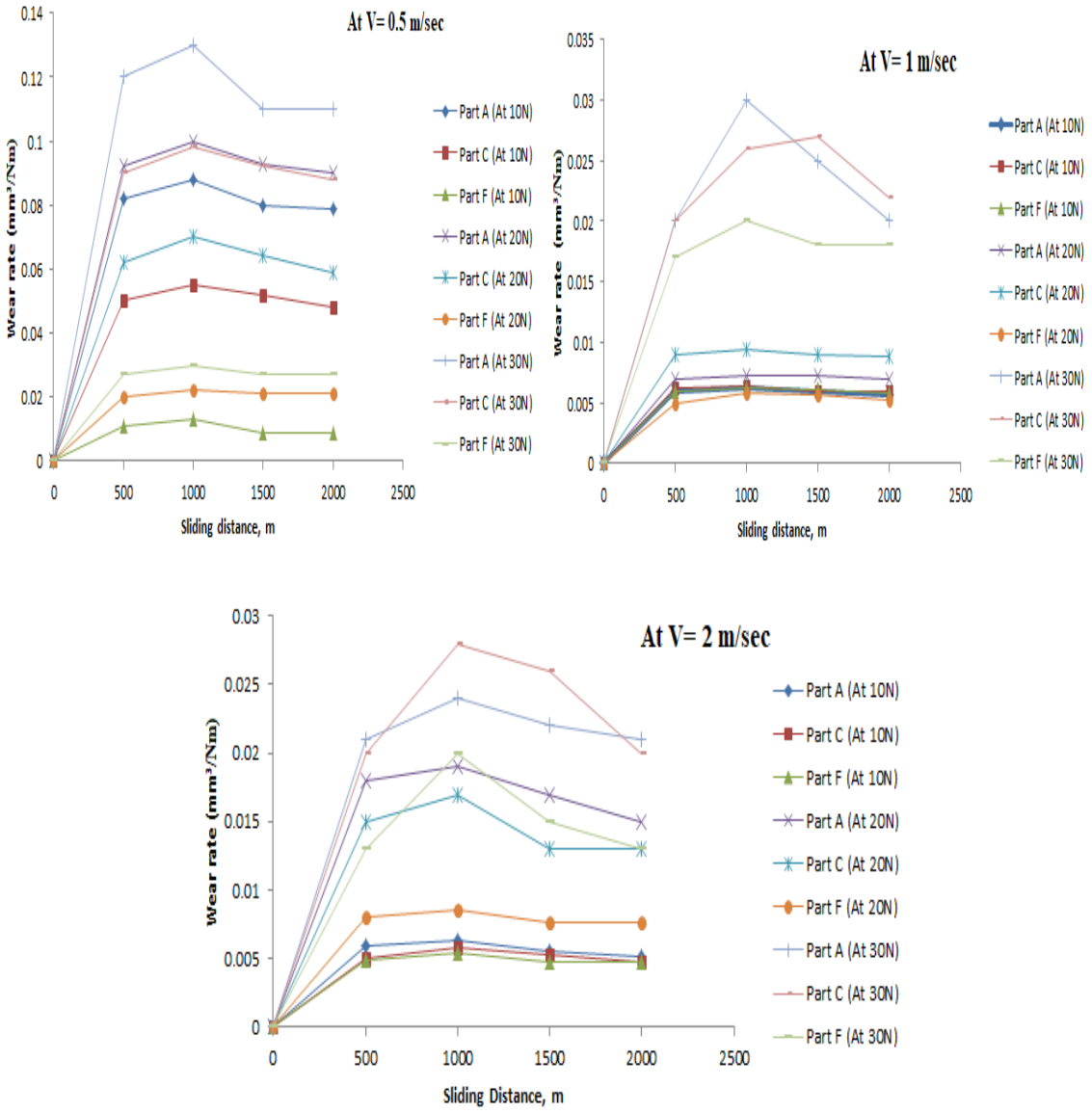

Figure 5.9 Graphs showing effect of sliding distance on wear rate of composites

5.4.4 SEM analysis of wear specimens

- ***At 0.5m/sec***

  The SEM images of both the specimens are shown in figure (6.6-6.8). As it can be seen from the images that wear surface is consists of fractured surfaces, pit formations, micro-cutting and ploughing. It was observed from figure 6.7, 6.8 that the size of the cracks as well as ploughing increases with increase in applied load. Also it can be seen that as compared to the base alloy and non-rare earth composites the size of cracks and plastic deformation is small. The pits formed in the base alloy shows that the wear rate is more in base alloy as compared to other two composites formed.

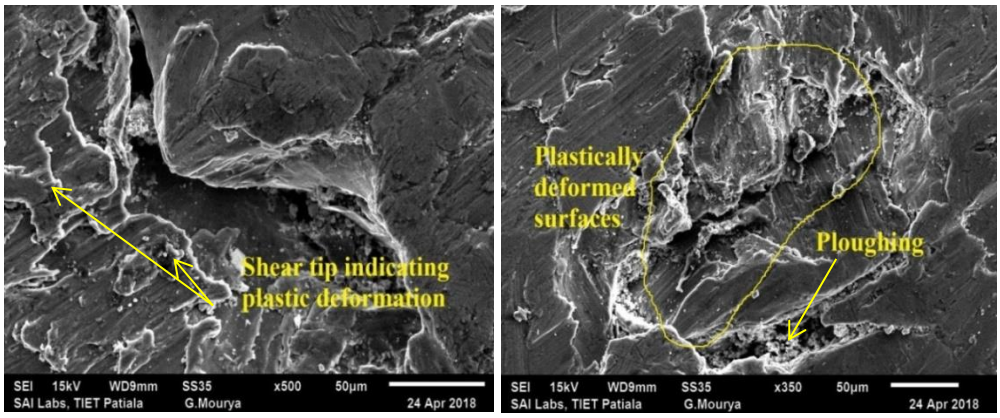

(a) (b)

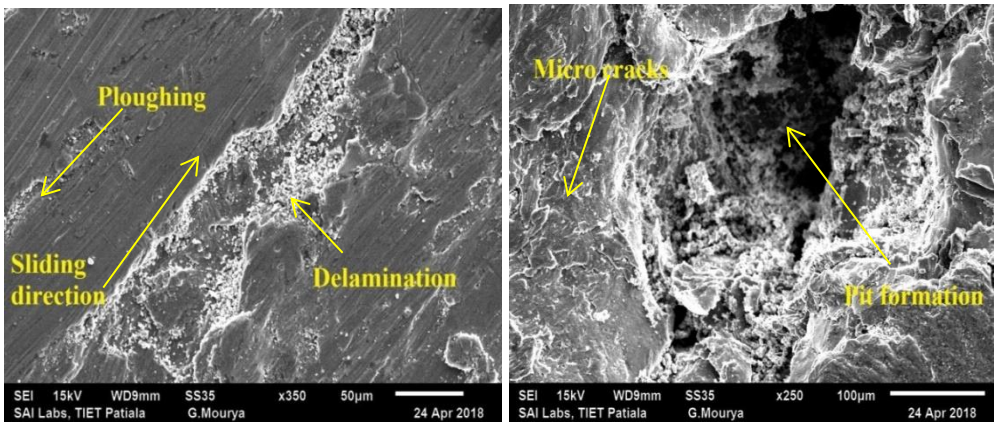

(c) (d)

Fig 5.10 SEM images of the wear specimens at sliding velocity 0.5 m/sec and load 10 N (a), (b) composite with Al_2O_3+Sic mixture (c) composite with Al_2O_3+Sic + CeO_2 mixture (d) Al-6061 base alloy

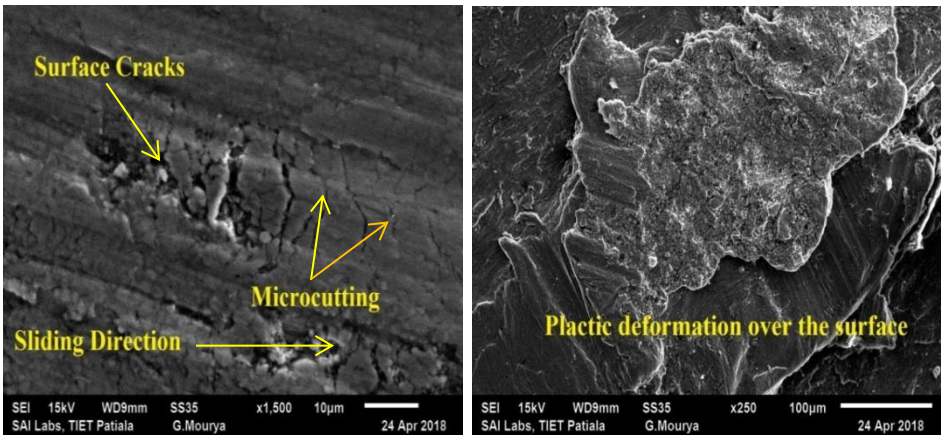

(a) (b)

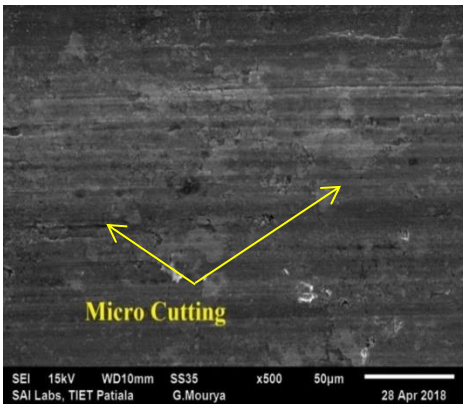

(c)

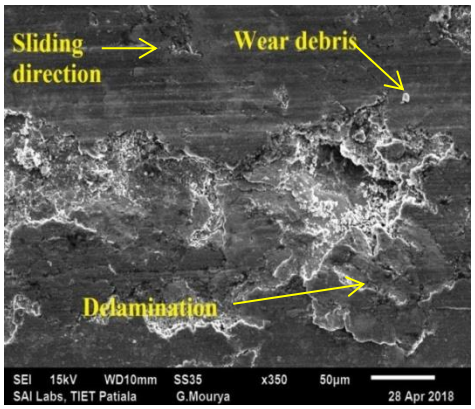

(d)

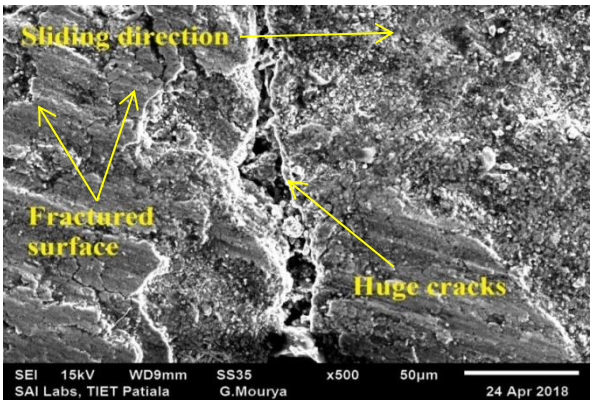

(e)

Fig 5.11 SEM images of the wear specimens at sliding velocity 0.5 m/sec and load 20 N (a), (b) composite with Al_2O_3+Sic mixture (c), (d) composite with Al_2O_3+Sic + CeO_2 mixture (e) Al-6061 base alloy

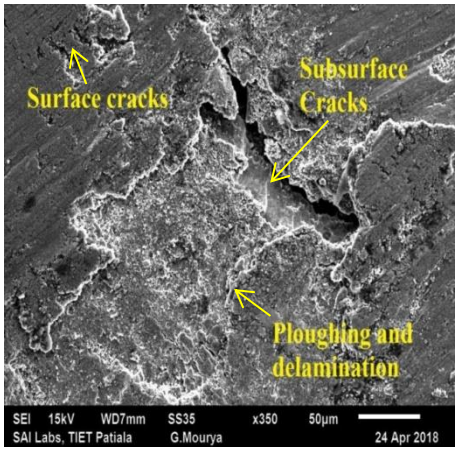

(a)

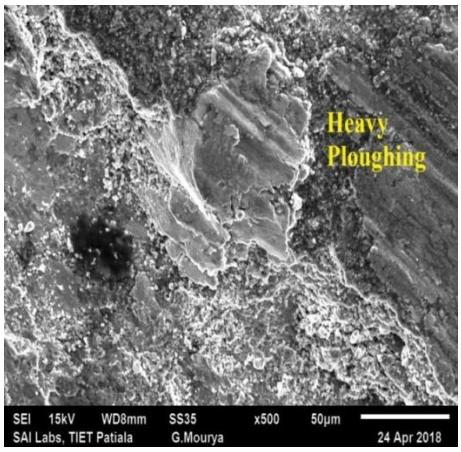

(b)

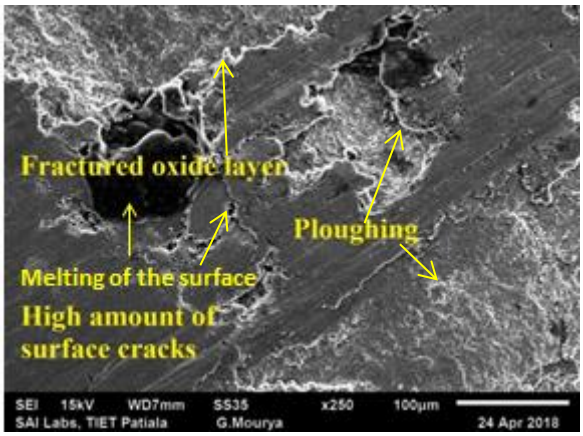

(c)

Fig 5.12 SEM images of the wear specimens at sliding velocity 0.5 m/sec and load 30 N (a) composite with Al_2O_3+Sic mixture (b) composite with Al_2O_3+Sic + CeO_2 mixture (c) Al-6061 base alloy

- ***At 1m/sec***

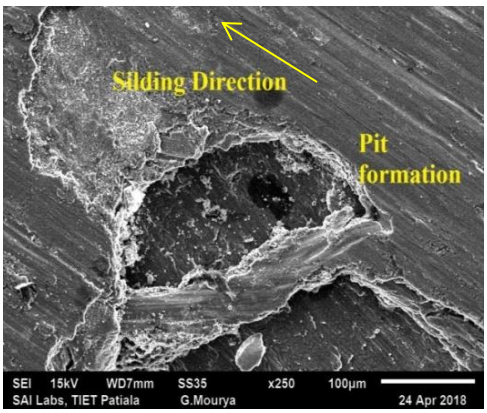

(a)

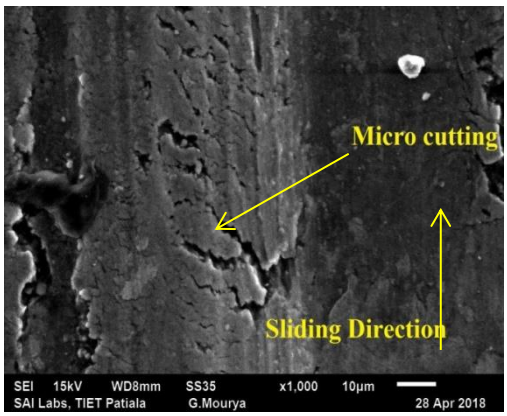

(b)

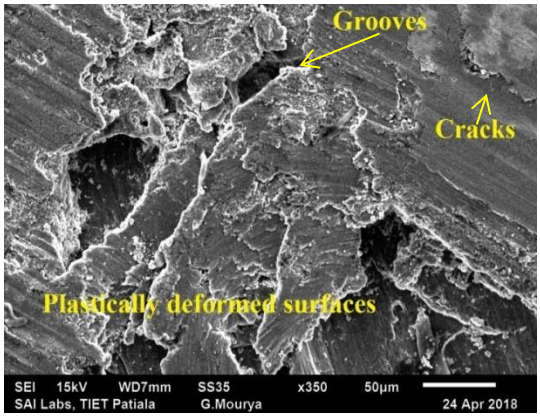

(c)

Fig 5.13 SEM images of the wear specimens at sliding velocity 1 m/sec and load 10 N (a) composite with Al_2O_3+Sic mixture (b) composite with Al_2O_3+Sic + CeO_2 mixture (c) Al-6061 base alloy

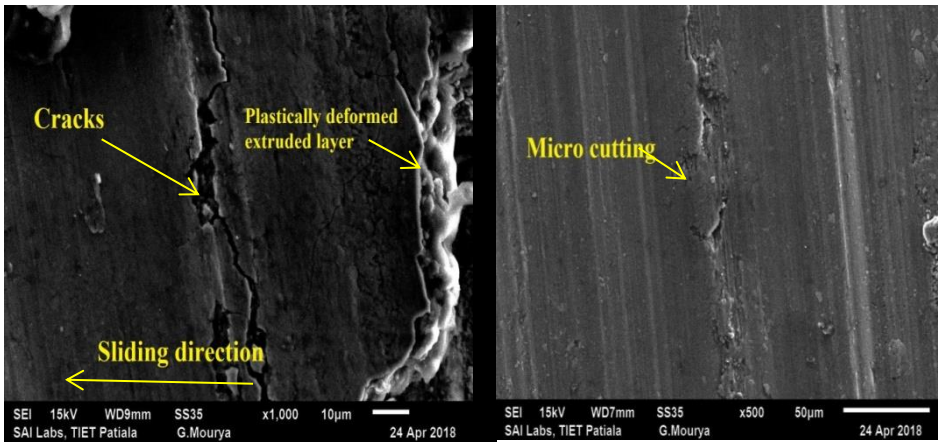

(a) (b)

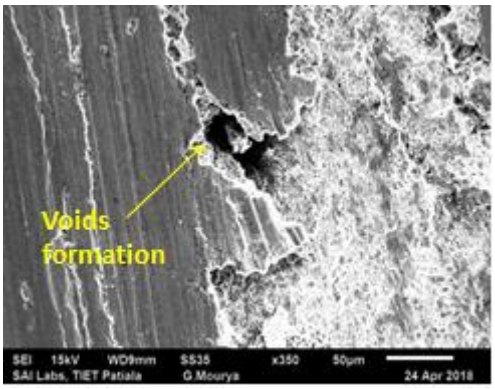

(c)

Fig 5.14 SEM images of the wear specimens at sliding velocity 1 m/sec and load 20 N (a) composite with Al_2O_3+Sic mixture (b) composite with Al_2O_3+Sic + CeO_2 mixture (c) Al-6061 base alloy

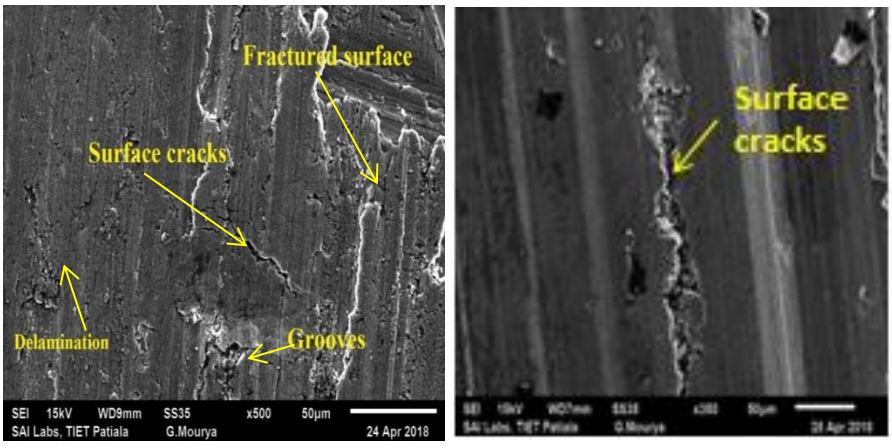

(a) (b)

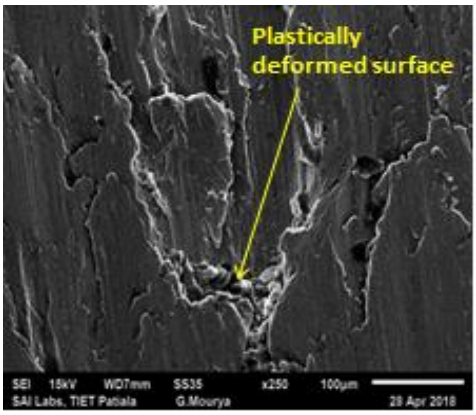

(c)

Fig 5.15 SEM images of the wear specimens at sliding velocity 1 m/sec and load 30 N (a) composite with Al_2O_3+Sic mixture (b) composite with Al_2O_3+Sic + CeO_2 mixture (c) Al-6061 base alloy

- ***At 2m/sec***

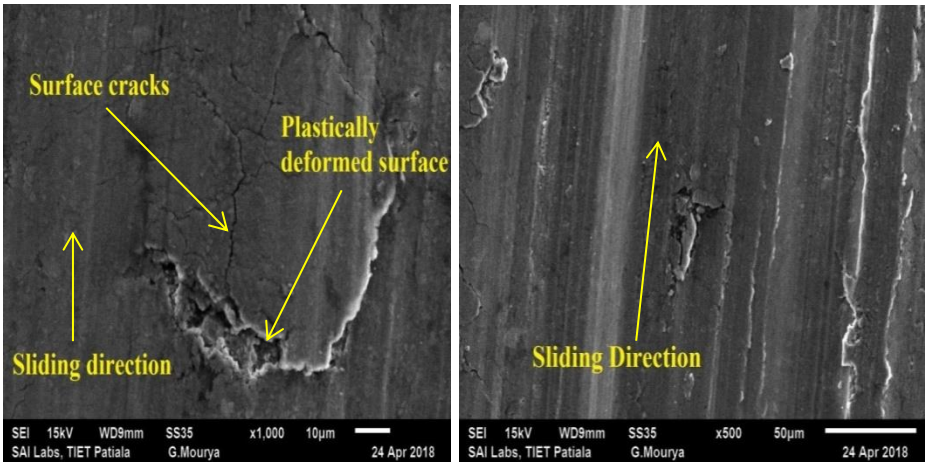

(a) (b)

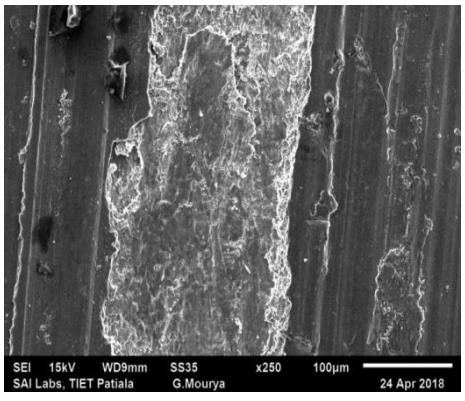

(c)

Fig 5.16 SEM images of the wear specimens at sliding velocity 2 m/sec and load 10 N (a) composite with Al_2O_3+Sic mixture (b) composite with Al_2O_3+Sic + CeO_2 mixture (c) Al-6061 base alloy

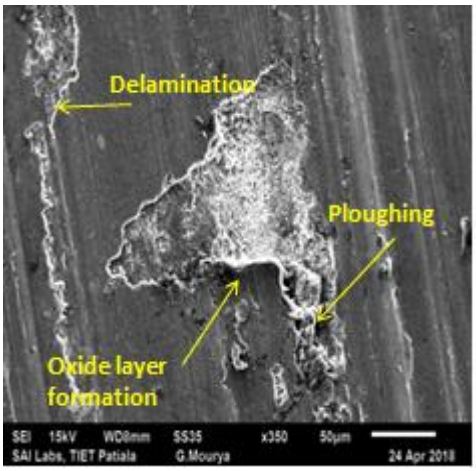

(a)

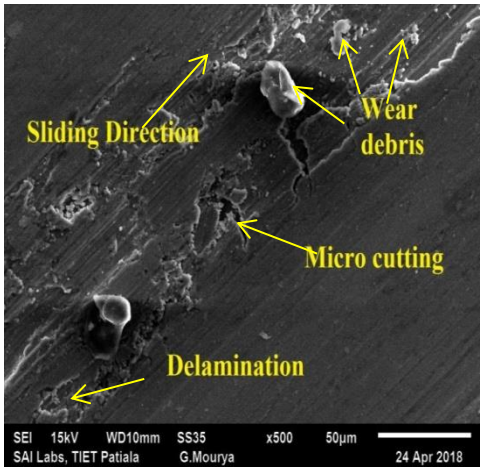

(b)

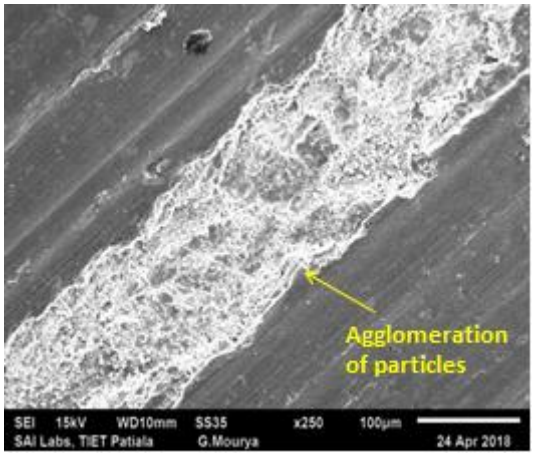

(c)

Fig 5.17 SEM images of the wear specimens at sliding velocity 2 m/sec and load 20 N (a) composite with Al_2O_3+Sic mixture (b) composite with Al_2O_3+Sic + CeO_2 mixture (c) Al-6061 base alloy

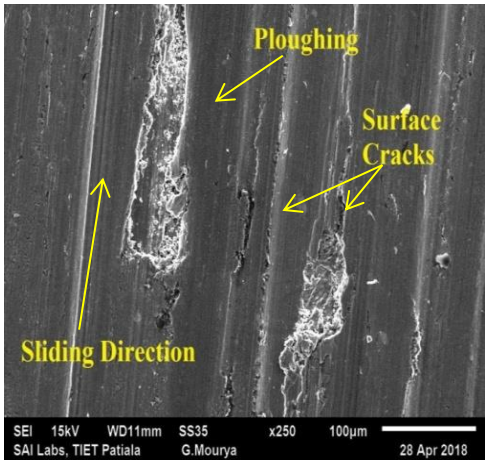

(a)

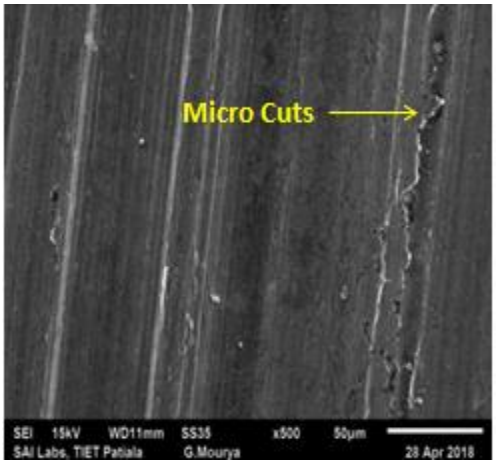

(b)

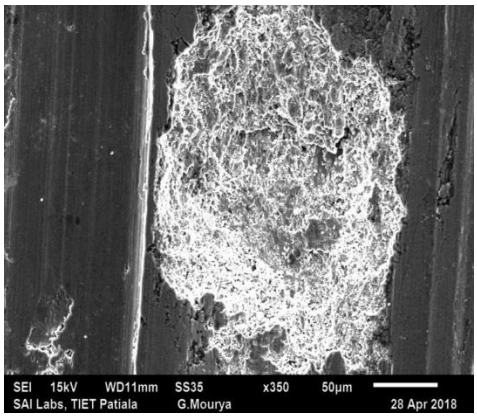

(c)

Fig 5.18 SEM images of the wear specimens at sliding velocity 2 m/sec and load 30 N (a) composite with Al_2O_3+Sic mixture (b) composite with Al_2O_3+SiC + CeO_2 mixture (c) Al-6061 base alloy

5.4.4 Tensile test results

The tensile specimens with and without rare earth oxides were prepared on the CNC-SIEMEN Test-Rig for comparing the tensile strength and %age elongation of the composites and the values obtained are specified in Table 5.3. It is evident from the true-stress strain curve for both with and without rare earth oxides that the composites with consist of CeO_2 have better load bearing capacity as compared to the composites having reinforcement of Al_2O_3/SiC.

The strengthening micromechanics of the matrix are influenced by the SiC/Al_2O_3 reinforcing particles. When particles reinforcement is introduced into a molten matrix of Al6061 aluminum alloy, there is usually a significant increase in the dislocation density throughout the composite due to the large difference in the coefficient of thermal expansion between the Al6061 aluminum matrix and SiC/Al_2O_3 particles reinforcement. Obviously in this work, the dispersion of SiC/Al_2O_3 is improved significantly with the addition of CeO_2 particulate additive. The dispersion of SiC/Al_2O_3 particles is equal to increasing the amount of SiC/Al_2O_3 reinforcing particles and reducing the size of the SiC/Al_2O_3. However, the composite having CeO_2 additive had a smaller grain matrix as compared to the composite without CeO_2 additive as indicated by the SEM micrographs.. The increase in tensile elongation can be due to the reduction in the size of matrix grain and the improvement of the SiC/Al_2O_3 particle dispersion (35).

Table 5.3 Tensile test results with percentage elongation

S.No	SAMPLES	UTS (Mpa)	% age improvement	% age elongation
(a)	Alloy+ 5%(Al_2O_3+ SiC)	30	-	2.0
(b)	Alloy+ 10%(Al_2O_3+ SiC)	54	80	2.1
(c)	Alloy+ 15%(Al_2O_3+ SiC)	73	35.18	6.8
(d)	Alloy+ 5%(Al_2O_3+ SiC) + 0.5% CeO_2(Rare earth)	89	21.9	7.2
(e)	Alloy+ 10%(Al_2O_3+ SiC) + 1.5% CeO_2(Rare earth)	102	14.6	10.0
(f)	Alloy+ 15%(Al_2O_3+ SiC) + 2.5% CeO_2(Rare earth)	123	20.6	11.5

A schematic diagram showing the tensile part machined for the test is shown below along with the tensile parts after testing :

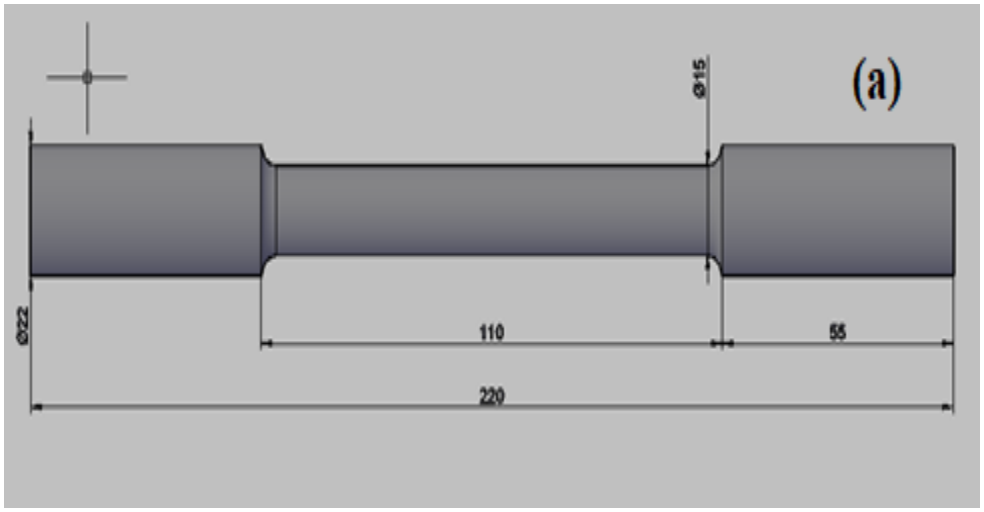

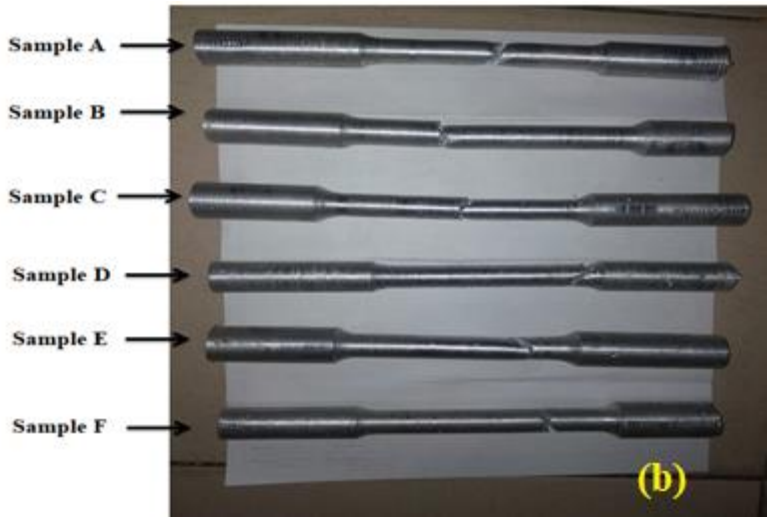

Figure 5.19 (a) Schematic for tensile specimen (b) Samples employed for tensile test

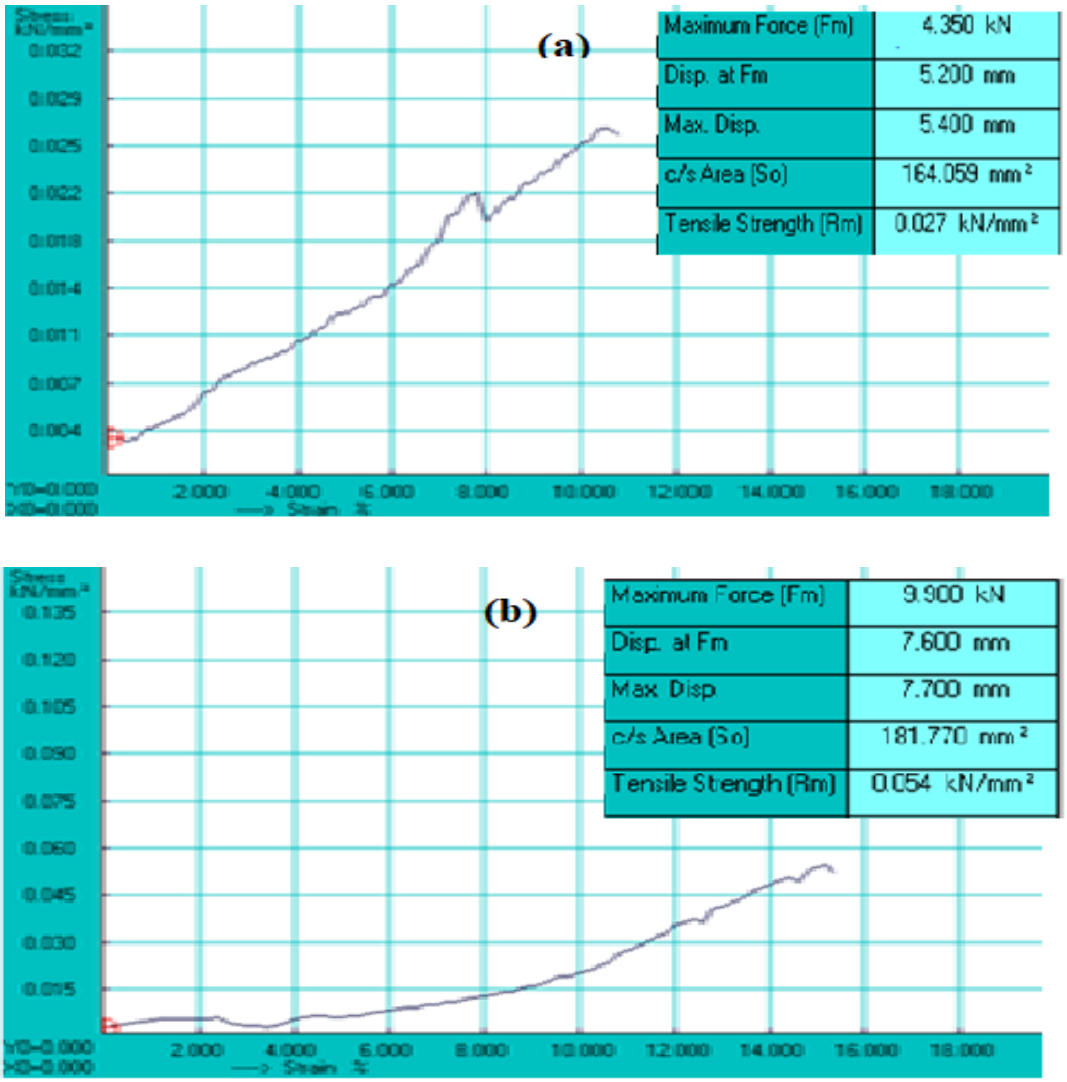

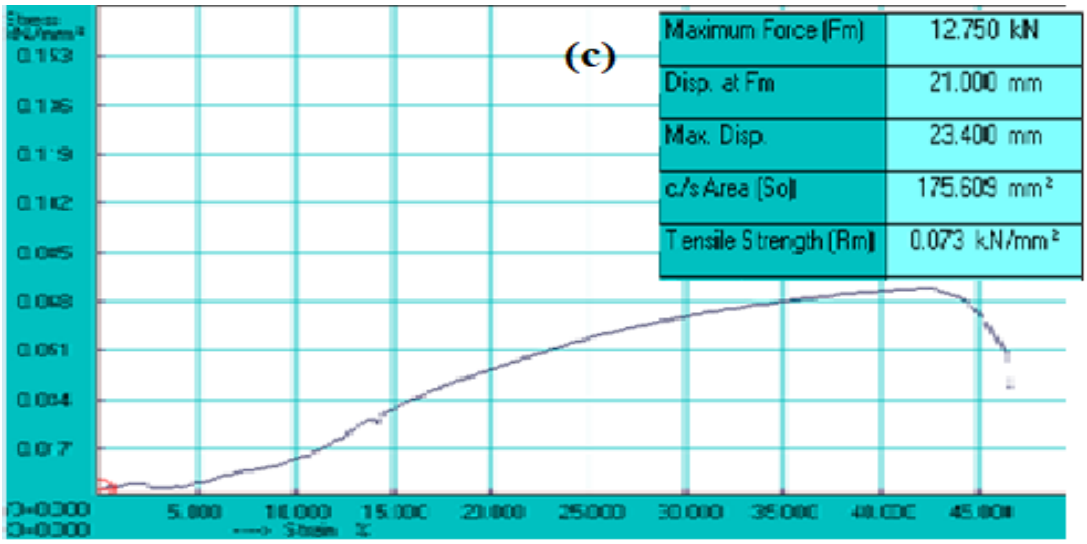
(c)
Maximum Force (Fm) 12.750 kN
Disp. at Fm 21.000 mm
Max. Disp. 23.400 mm
c/s Area (So) 175.609 mm²
Tensile Strength (Rm) 0.073 kN/mm²

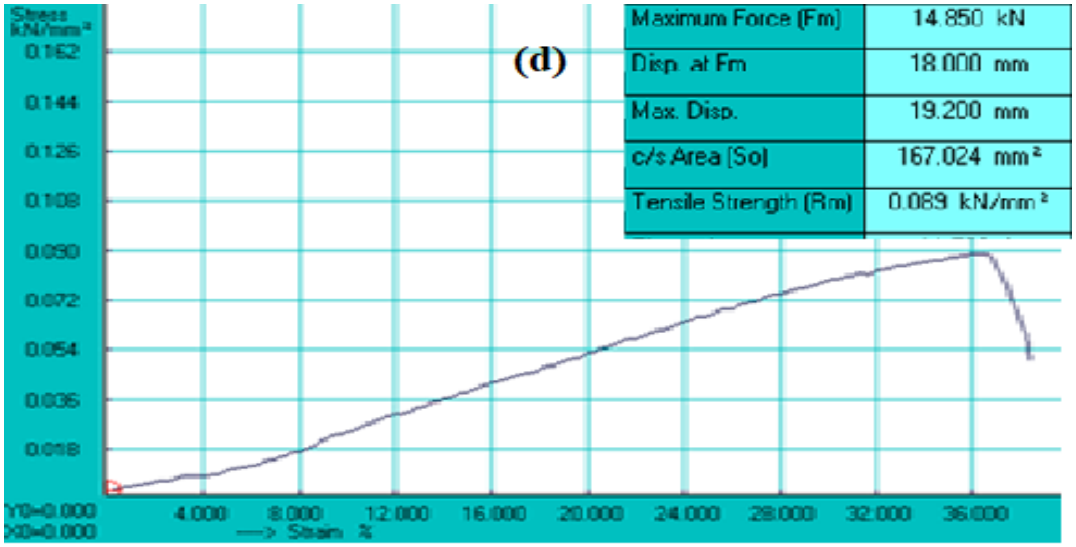
(d)
Maximum Force (Fm) 14.850 kN
Disp. at Fm 18.000 mm
Max. Disp. 19.200 mm
c/s Area (So) 167.024 mm²
Tensile Strength (Rm) 0.089 kN/mm²

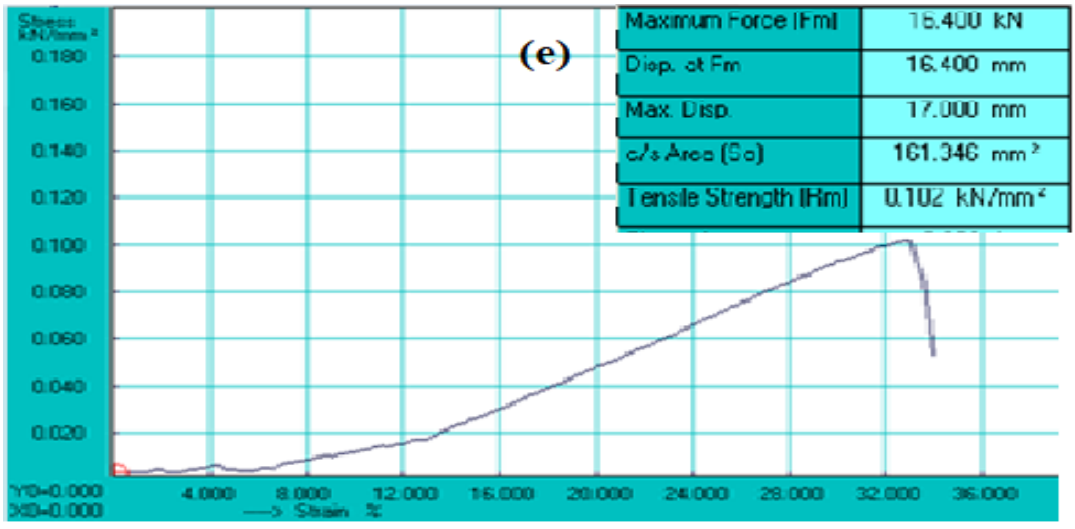
(e)
Maximum Force (Fm) 16.400 kN
Disp. at Fm 16.400 mm
Max. Disp. 17.000 mm
c/s Area (So) 161.346 mm²
Tensile Strength (Rm) 0.102 kN/mm²

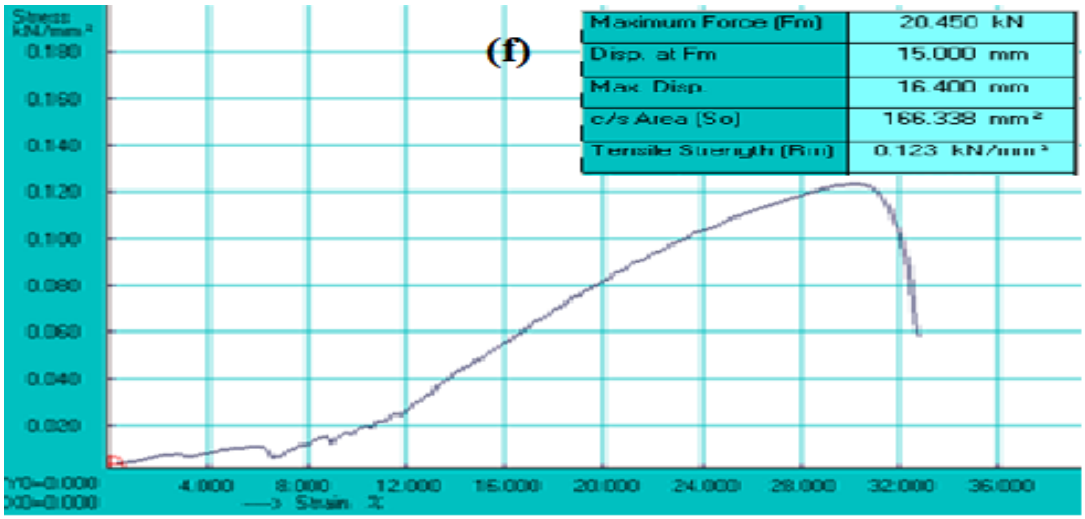

Figure 5.20. Tensile test results of composite samples showing stress vs strain relationship

As it can be seen from the graphs the value of maximum force required to break the specimen increased as the percentage of reinforcement increases and becomes maximum in part 'f' which tends to increase the ultimate tensile strength of the composite. It shows that by addition of 2.5% CeO_2 the value of tensile strength increases. The weakest point of a tensile specimen is mostly the middle part, when it is subjected to tensile test, so the specimen breaks from the centre but as it can be seen from figure 5.19 (b) that most of the specimens have breaked away from the middle which can be due to presence of certain defects, particle concentration or minute impurities which may cause the fracture not from the middle of the specimen. The test reveals that UTS of composites increases from 30 Mpa to 123 Mpa after addition of rare earth metal. From figure 5.21 it can be observed that on comparing non-rare earth composites with rare earth composites the value of tensile strength is more in case of rare earth composites. Also the value of percentage elongation also increases. The increase in both the properties of composites shows that the composites generated have homogeneous composition. Better homogeniety in mixture results in better properties. From the literature review it was observed that in some cases with increase in reinforcement percentage the value of percentage elongation decreases because with the addition of reinforcement particles the resistance in flowabilty of aluminum matrix decreases and there is a reduction in ductility of the alloy (13). But in this case increase in %age elongation can be seen by addition of rare earth metal into the matrix composition which could be due to better strain hardening and better grain refinement (can be seen through various SEM microstructure images) that not only increases the UTS of the composites but also increases the value of %age

elongation of the composites. The combine effects of %age reinforcement addition on the ultimate tensile strength (UTS) and percentage elongation on both the composites i.e. Non-rare earth (NRE) as well as rare earth (RE) composites is shown below.

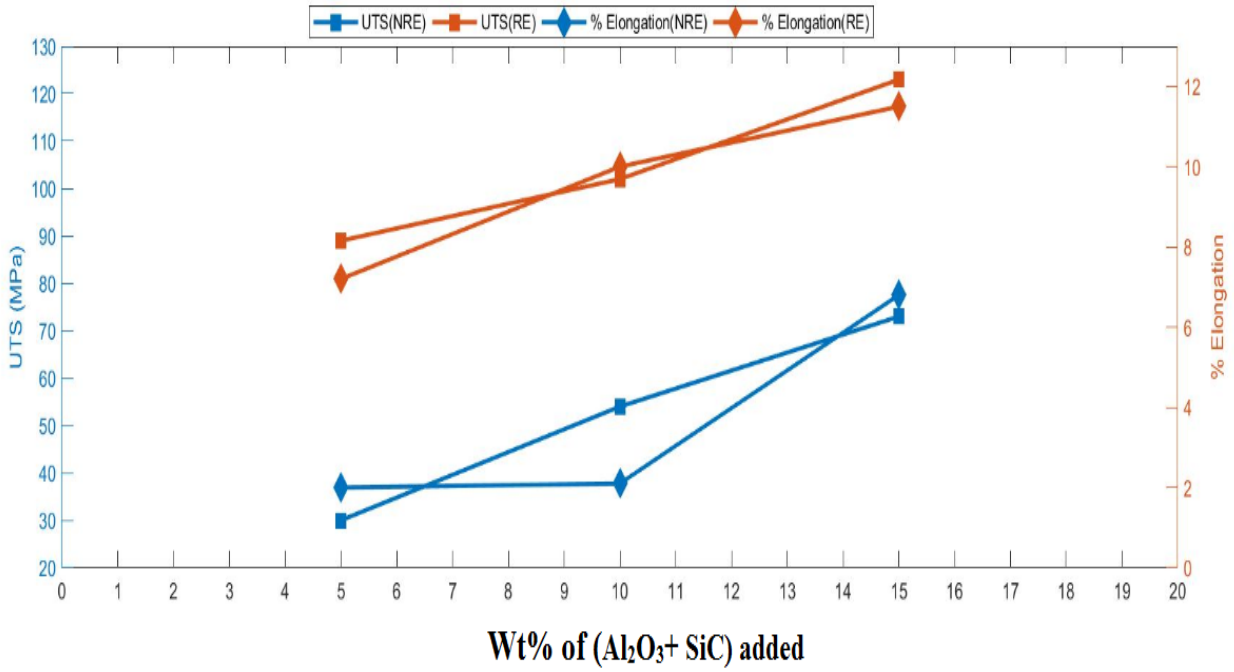

Figure 5.21 Combined effect of weight percentage of reinforcement added on UTS and % elongation of the composites

Chapter 6

Conclusions

The hybrid composite of Al6061 alloy reinforced with Al_2O_3+ Sic+ CeO_2 was successfully fabricated using stir casting technique and characterizations of composites were carried out. Major conclusions drawn from the work are:

1) Micro hardness (using Vicker's hardness tester) value of the base alloy was increased by 17.02% by addition of 2.5% rare earth along with (Al_2O_3+Sic) mixture and as compared to non-rare earth element (Alloy+ 15%(Al_2O_3+ Sic) mixture the hardness increased by 13.70%. Whereas the value of Rockwell hardness of the base alloy increased by 33.80% by addition of rare earth and as compared to non-rare the hardness increased by 16.32%.
2) Under different values of normal loads and sliding velocities investigated, the composite with a mixture of rare earth was found to have decrease in wear rate under all conditions. The major factors that contributed to the reduction in wear rate were refinement in the microstructure resulting in increase in hardness and hence greater work hardening capabilities.
3) It was found that the maximum wear rate occurred at higher load and lower velocities. Also it was found that during progressive wear testing the wear rate is maximum in the initial stage but with the increase in sliding distance, the wear rate tends to reduce and then become steady.
4) The major wear mechanism at higher velocities was found to be plastic deformation along with delamination and cracks. It was seen from the SEM images of wear samples that the reduction in cracks was there with the addition of rare earth as compared to base and non- rare earth composites. The plastic deformation tends to lower down.
5) SEM images shows the pattern of microstructure Al_2O_3 particles to be very fine as compared to the particle pattern of the Sic. Very fine and smooth structure of hybrid composites was seen using rare earth oxides as reinforcement element.
6) XRD analysis shows the presence of presence of various phases like SiO_2,$Mg(CO_3)$,$FeAl_2Si$ in hybrid composites The XRD study of CeO_2 modified aluminium alloy showed that presence of Al, SiO_2, Mg_5Si_6, MgO, Ce_2 O_3 and

$Ce_{11}O_{20}$ phases . The presence of Ce_2 O_3 and $Ce_{11}O_{20}$ indicated successful addition of the cerium oxide as a rare earth oxides in the aluminium alloy Al-6061

7) From EDS analysis it was clear that the oxygen and carbon peaks were observed. It is very much confirms from the EDS analysis that aluminum SiC particles and cerium oxide are present within the composites. Therefore, these results of SEM indicated that successful incorporation of Hybrid ceramics Al_2O_3/SiC/CeO_2-reinforced Al-matrix composites produced by the stir casting process.
8) The Ultimate tensile strength (UTS) of hybrid composites tends to improve by addition of reinforcements. UTS increased from 30Mpa value of non-rare earth composite to 123Mpa value after addition of rare earth. Percentage elongation was also seen to be increased with increase in amount of reinforcement and was seen to rise from 2.0% to 11.5%.

REFERENCES

1) Oluwatosin Bodunrin M, Kanayo Alaneme K, Heath Chown L (2015), Aluminum matrix hybrid composites: a review of reinforcement philosophies; mechanical corrosion and tribological characteristics, Journal of material research of technology, 4(4), 434-445.
2) Kok M (2005), Production and mechanical properties Al_2O_3 particle- reinforced 2024 aluminum alloy composites, Journal of material processing technology, 161, 381-387.
3) Surappa M K (2003), Aluminum matrix composites: Challenges and opportunities, Sadhana, 28, 319-334.
4) Alaneme K. K and Bodunrin M.O (2011), Corrosion behavior of alumina reinforced aluminum 6063 metal matrix composites, Journal of mineral & materials characterization & engineering, 10(12), 1153-1165.
5) Rajan T.P.D., Pillai, R.M., Pai, B.c., Satyanarayana, K.G., Rohatgi, P.k (2007), Fabrication and characterization of Al-7Si-0.35Mg/fly ash metal matrix composite processed by different stir casting routes, Composite science and technology, 67(15-16), 3369-3377.
6) Narayan S, Rajeskannan A (2017), Hardness, tensile and impact behavior of hot forged aluminum MMC, Journal of material research and technology, 6(3), 2013-2019.
7) Huang X F, Changxia L, Musen Li and Jianhua Z (2005), Effect of rare earth on the microstructure and properties of Mg-5Al-1Si alloy, Rare metal materials and engineering, 2005, 34(5), 367-370.
8) Tjong SC (2014), Processing and deformation characteristics of metals reinforced with ceramic nanoparticles. In: Tjong S-C, editor, nanocrystalline materials (internet). 2nd edition. Oxford: Elsevier, 269-304.
9) B. Vijaya Ramanath, C. Elanchezhian, RM. Annamalai, S. Aravind, T. Sri Ananda Atreya, V. Vignesh and C. Subramaniam (2014), Aluminum metal matrix composites-a review, Advance material science, 38, 55-60.
10) Prasad S.V, Asthana R (2004), Aluminum metal- matrix composites for automotive applications: tribological considerations, Tribology letters, 17(3), 445-453.
11) Sijo M.T, Jayadevan K R (2016), Analysis of stir cast aluminum silicon carbide metal matrix composite: a comprehensive review, Procedia technology, 24, 379-385.

12) Raj R, Thakur G D (2016), Qualitative and quantitative assessment of microstructure in Al-B_4C metal matrix composite processed by modified stir casting technique, Archives of civil and mechanical engineering, 16, 949-960.

13) Singh G, Goyal S (2016), Microstructure and mechanical behavior of Al6082-T6/SiC/B_4C- based aluminum hybrid composites, Particulate science and technology, 1-8.

14) Arora H.S., Singh. H and Dhindaw B.K (2013), Wear behavior of a Mg alloy subjected to friction stir processing, Journal of wear, 303, 65-77.

15) David Raja Selvam. J (2013), Synthesis and characterization of aluminum 6061-fly ash-SiC- composites by stir casting and compocasting methods, Energy procedia, 34, 637-646.

16) Xihua Z, Changxia L, Musen LI and Jianhua Z (2008), Research on toughening mechanisms of alumina matrix composites material improved by rare earth additive, Journal of rare earth, 26(3), 367-370.

17) Samuel Ratan Kumar P.S, Robinson Smart D.S, John Alexis S (2017), Corrosion behavior of aluminum metal matrix reinforced with multi-wall carbon nanotube, Journal of Asian ceramic societies, 5, 71-75.

18) James J.S, Venkatesan .K, Kuppan P and Ramanujam. R (2014), Hybrid aluminum metal matrix composites reinforced with SiC and TiB_2, Procedia engineering, 97, 1018-1026.

19) Shojaeefard M.H, Akbari M, Asadi P and Khalkhali A (2017), The effect of reinforcement type on the microstructure, mechanical properties and wear resistance of Al356 matrix composites produced by FSP, Int. J of advance manufacturing technology, 91 (1-4), 1391- 1407

20) Rebba B, Ramanaiah N (2014), Evaluation of mechanical properties of aluminum alloy (Al2024) reinforced with molybdenum disulphide (MOS_2) metal matrix composites, Procedia materials sciences, 6, 1161-1169.

21) Wang Xu, Chen G, Yang W, Hussain M, Wang C, Gaohui Wu and Jiang D (2011), Effect of Nd content on microstructure and mechanical properties of Gr/Al composite, Material science and engineering A, 528, 8212-8217.

22) Padmavathi K.R, Dr. R. Ramakrishnan (2014), Tribolological behavior of aluminum hybrid metal matrix composite, Procedia engineering, 97, 660-667.

23) Kumar Siddesh, Ravindranath VM and Shiva Shankar GS (2014), Mechanical and wear behavior of aluminum metal matrix hybrid composites, Procedia materials science, 5, 908-917.

24) Kumar Pal. Manoj, Singh S, Kalia. R and Ghosh. A (2015), Identification of optimum composition and mechanical properties of Al-Ni metal matrix composites, Journal of mineral and materials characterization and engineering , 3, 326-334.
25) Siva Prasad. D, Shoba.C and Ramanaiah. N (2014), Investigations on mechanical properties of aluminum hybrid composites, Journal of material research and technology, 3(1), 79-85.
26) Prasantha Kumar H.G, Anthony Xavior. M (2017), Assessment of mechanical and tribological properties of Al-2024–Sic-graphene hybrid composites, Procedia engineering, 174, 992-999.
27) Li. Hongying, Gao. Z, Yin. H, Jiang. H, Xiongjie Xu and Bin. J (2013), Effects of Er and Zr additions on precipitation and recrystallization of pure aluminum, Scripta materialia, 68, 59-62.
28) Rashed F.S, Mahmoud. T.S (2009), Prediction of wear behavior of A356/SiC MMCs using neural networks, Tribology international, 42, 642-648.
29) Sushil. M, Kumar Vinod & Kumar Harmesh (2015), Experimental investigation and optimization of process parameters of Al/SiC MMCs finished by abrasive flow machining, Materials and manufacturing processes, 30, 902-911.
30) Dr. P.V.Krupakara, Ravikumar. H. R (2015), Corrosion characterization of aluminum 6061/ Red mud metal matrix composites in sea water, International journal of advance research in chemical science, 2(6), 52-55.
31) Huang Fen, Xizhong. A, Zhang. Y and A.B. Yu (2017), Multi-particle FEM simulation of 2D compaction on binary Al/SiC composites powders, Powder technology, 314, 39-48.
32) Soorya Prakash. K, Balasundar. P, Nagaraja. S, Gopal. P.M and Kavimani. V (2016), Mechanical and wear behavior of Mg-SiC-Gr hybrid composites, Journal of magnesium and alloys, 4, 197-206.
33) K Sharma. Vipin, Singh R.C and Chaudhary. R (2017), Effect of fly ash particles with aluminum melt on the wear of aluminum metal matrix composites, Engineering science and technology, an international journal, 20, 1318-1323.
34) Liu Youming, Li Wenyi, Xu. B, Cai. X, Liuhi Li and Chen. Q (2004), The behavior and effect of rare earth CeO_2 on In-situ TiC/Al composite, Metallurgical and materials transactions, 35A, 2511-2515.
35) Jing Xue, Jun Wang, Yanfeng Han, Pan Li, Baode Sun (2011), Effects of CeO_2 additive on the microstructure and mechanical properties of in-situ TiB_2/Al composites, Journal of alloy and composites, 509, 1573-1578.